Cellular/Molecular

Meclizine and Metabotropic Glutamate Receptor Agonists Attenuate Severe Pain and Ca^{2+} Activity of Primary Sensory Neurons in Chemotherapy-Induced Peripheral Neuropathy

John Shannonhouse,[1] Matteo Bernabucci,[3] Ruben Gomez,[1] Hyeonwi Son,[1] Yan Zhang,[1] Chih-Hsuan Ai,[1] Hirotake Ishida,[1] and Yu Shin Kim[1,2]

[1]Department of Oral & Maxillofacial Surgery, School of Dentistry, [2]Programs in Integrated Biomedical Sciences, Translational Sciences, Biomedical Engineering, Radiological Sciences, University of Texas Health Science Center at San Antonio, San Antonio, Texas 78229, and [3]Department of Neuroscience and Cell Biology, Rutgers Robert Wood Johnson Medical School, Piscataway, NJ 08854

Chemotherapy-induced peripheral neuropathy (CIPN) affects ~68% of patients undergoing chemotherapy, causing debilitating neuropathic pain and reducing quality of life. Cisplatin is a commonly used platinum-based chemotherapeutic drug known to cause CIPN, possibly by causing oxidative stress damage to primary sensory neurons. Metabotropic glutamate receptors (mGluRs) are widely hypothesized to be involved in pain processing and pain mitigation. Meclizine is an H1 histamine receptor antagonist known to have neuroprotective effects, including an anti-oxidative effect. Here, we used a mouse model of cisplatin-induced CIPN using male and female mice to test agonists of mGluR8 and Group II mGluR as well as meclizine as interventions to reduce cisplatin-induced pain. We performed behavioral pain tests, and we imaged Ca^{2+} activity of the large population of dorsal root ganglia (DRG) neurons *in vivo*. For the latter, we used a genetically-encoded Ca^{2+} indicator, Pirt-GCaMP3, which enabled us to monitor different drug interventions at the level of the intact DRG neuronal ensemble. We found that CIPN increased spontaneous Ca^{2+} activity in DRG neurons, increased number of Ca^{2+} transients, and increased hyper-responses to mechanical, thermal, and chemical stimuli. We found that mechanical and thermal pain caused by CIPN was significantly attenuated by the mGluR8 agonist, (S)−3,4-DCPG, the Group II mGluR agonist, LY379268, and the H1 histamine receptor antagonist, meclizine. DRG neuronal Ca^{2+} activity elevated by CIPN was attenuated by LY379268 and meclizine, but not by (S)−3,4-DCPG. Furthermore, meclizine and LY379268 attenuated cisplatin-induced weight loss. These results suggest that Group II mGluR agonist, mGluR8 agonist, and meclizine are promising candidates as new treatment options for CIPN, and studies of their mechanisms are warranted.

Key words: chemotherapy-induced neuropathy; chronic pain; GCaMP calcium imaging; *in vivo* imaging; meclizine; primary sensory neuron

Significance Statement

Chemotherapy-induced peripheral neuropathy (CIPN) is a painful condition that affects most chemotherapy patients and persists several months or longer after treatment ends. Research on CIPN mechanism is extensive but has produced only few clinically useful treatments. Using *in vivo* GCaMP Ca^{2+} imaging in live animals over 1800 neurons/dorsal root ganglia (DRG) at once, we have characterized the effects of the chemotherapeutic drug, cisplatin and three treatments that decrease CIPN pain. Cisplatin increases sensory neuronal Ca^{2+} activity and develops various sensitization. Metabotropic glutamate receptor (mGluR) agonist, LY379268 or the H1 histamine receptor antagonist, meclizine decreases cisplatin's effects on neuronal Ca^{2+} activity and reduces pain hypersensitivity. Our results and experiments provide insights into cellular effects of cisplatin and drugs preventing CIPN pain.

Received May 21, 2021; revised June 2, 2022; accepted June 22, 2022.

Author contributions: M.B. and C.-H.A. designed research; M.B., R.G., and H.S. performed research; J.S., R.G., Y.Z., and H.I. contributed unpublished reagents/analytic tools; Y.S.K., J.S., M.B., R.G., H.S., Y.Z., H.I., and C.-H.A. analyzed data; Y.S.K. and J.S. wrote the first draft of the paper; Y.S.K. edited the paper; Y.S.K. wrote the paper.

This work was supported by National Institutes of Health Grants R01DE026677, R35DE030045, and R01DE031477 (to Y.S.K.), UTHSCSA startup fund (Y.S.K.), and a Rising STAR Award from University of Texas system (Y.S.K.).

The authors declare no competing financial interests.

Correspondence should be addressed to Yu Shin Kim at kimy1@uthscsa.edu.

https://doi.org/10.1523/JNEUROSCI.1064-21.2022

Introduction

Chemotherapy-induced peripheral neuropathy (CIPN) is a side effect of chemotherapy, which affects ~68% of patients, causing severe neuropathic pain that may persist for six months or longer in ~30% of patients who have undergone chemotherapy (Quasthoff and Hartung, 2002; Seretny et al., 2014; Addington and Freimer, 2016; Cioroiu and Weimer, 2017; Flatters et al., 2017). Cisplatin is a platinum-based chemotherapeutic agent that inhibits tumor growth by crosslinking DNA

nucleotides (Greystoke et al., 2017; Armstrong-Gordon et al., 2018), and which is widely used to treat cancer in various locations including lung, stomach, and head (Seretny et al., 2014; Calls et al., 2020). There have been extensive studies on strategies to reduce neuropathic pain and to understand its mechanisms at the level of individual cells, using *in vitro* dorsal root ganglia (DRG) explants and histologic analysis in animal models (Quasthoff and Hartung, 2002; Jaggi and Singh, 2012; Addington and Freimer, 2016; Cioroiu and Weimer, 2017). However, because of a lack of suitable tools and techniques, CIPN has not been studied *in vivo* at the level of an intact DRG neuronal ensemble, leaving an important gap in the understanding of CIPN mechanisms necessary to develop better therapeutics.

There are numerous nonmutually exclusive proposed mechanisms for CIPN caused by platinum-based chemotherapeutic drugs (Jaggi and Singh, 2012). These potential mechanisms including mitochondrial malfunction and cytoplasmic calcium unbalance (Melli et al., 2008), alteration of potassium channel subtype expression (Descoeur et al., 2011), upregulation of transient receptor potential vanilloid receptors (Anand et al., 2010; Ta et al., 2010), endoplasmic reticulum (ER) stress (Nawrocki et al., 2005; Yi et al., 2020), primary sensory neuron senescence (Calls et al., 2021), and oxidative stress via mitochondrial disruption generating reactive oxygen species (ROS; Joseph et al., 2008; Gorgun et al., 2017; Khasabova et al., 2019). ROS produced by mitochondria are normally broken down by the superoxide dismutase pathway (McCord and Fridovich, 1988). An SOD mimetic drug, calmangafodipir, reduced CIPN symptoms caused by oxaliplatin, a platinum-based drug (Glimelius et al., 2018). Of particular relevance to our work here, physiological changes associated with cisplatin-induced CIPN overlap extensively with known mechanisms of inflammatory pain (Hu et al., 2018; Quintão et al., 2019; Y. Zhu et al., 2019).

Concomitant administration of anti-inflammatory drugs with cisplatin has reduced CIPN-induced neuropathic pain both in animal models and in clinical trials (Glimelius et al., 2018; Khasabova et al., 2019). *In vivo* DRG imaging may be a particularly useful strategy for studying how concomitant drug administration modifies the effect of cisplatin on primary sensory neurons. All mGluRs except mGluR6 are found on central and/or peripheral neurons known to be involved in nociception, and are known to affect pain (Yang and Gereau, 2002, 2003; Marabese et al., 2007; Chiechio et al., 2010; Jaggi and Singh, 2012; Mazzitelli et al., 2018; Pereira and Goudet, 2018). In particular, inflammatory pain is attenuated by Group II mGluRs (mGluR2 and mGluR3) and Group III mGluRs (mGlurR4, mGluR7, and mGluR8; Zammataro et al., 2014; Mazzitelli et al., 2018; Pereira and Goudet, 2018), and is enhanced or modulated by Group I mGluRs (mGluR1 and mGluR5; Bhave et al., 2001; Karim et al., 2001; Zammataro et al., 2014; Radwani et al., 2017; Mazzitelli et al., 2018; Pereira and Goudet, 2018; Masuoka et al., 2020). Thus, metabotropic glutamate receptors (mGluRs), especially Groups II and III, are promising therapeutic targets for CIPN-induced neuropathic pain (Mazzitelli et al., 2018; Pereira and Goudet, 2018).

Meclizine is also an attractive candidate for reducing CIPN caused by platinum-based drugs. Meclizine is an H1 receptor antagonist and a pregnane X receptor agonist in mice shown to be neuroprotective in animal models of conditions as diverse as Huntington's (Gohil et al., 2011), Parkinson's (Hong et al., 2016), and hypoxia (Zhuo et al., 2016). Meclizine protects cultured DRG primary sensory neurons from cisplatin-induced damage by enhancing pentose phosphate pathway activity, enhancing NADPH production, and improving clearance of DNA damage (Gorgun et al., 2017). Furthermore, meclizine shifts retinal ganglion cells toward the glycolysis metabolism pathway and away from the mitochondrial respiratory pathway (J. Zhu et al., 2020), suggesting that meclizine could protect against cisplatin-induced oxidative stress and mitochondrial toxicity.

In this study, we used mechanical and thermal pain behavioral assays and confocal microscopic imaging with the genetically-encoded fluorescent calcium indicator, Pirt-GCaMP3, to investigate cisplatin-based CIPN-induced neuropathic pain *in vivo* at the level of an intact ensemble comprising the large DRG primary sensory neuronal population. We found that cisplatin induced mechanical and thermal hypersensitivity in pain behavioral assays, increased levels of spontaneous Ca^{2+} activity in DRG primary sensory neurons, and increased Ca^{2+} responses to mechanical, thermal, and chemical stimuli. mGluR8 agonist (S)−3,4-DCPG, Group II mGluRs (mGluR2 and mGluR3) agonist LY379268, and histamine H1 receptor antagonist, meclizine, each attenuated cisplatin-induced pain in behavioral assays. Furthermore, LY379268 and meclizine attenuated spontaneous calcium activity in DRG neurons *in vivo*. Finally, meclizine and LY379268 reduced cisplatin-induced weight loss.

Materials and Methods

Animals

All experiments were performed in compliance with policies and procedures of the Institutional Animal Care and Use Committee at University of Texas Health Science Center at San Antonio (UTHSA) and in accordance with National Institutes of Health and American Association for Accreditation of Laboratory Animal Care. Pirt-GCaMP3 mice (Kim et al., 2014, 2016) on a C57BL/6J background or C57BL/6J mice (The Jackson Laboratory) were used in all experiments. Pirt-GCaMP3 mice used in experiments were all heterozygous. Both males and females were used. All animals were at least eight weeks old, were kept in a 14/10 h light/dark cycle, and were provided *ad libitum* access to food and water.

Drugs and drug treatment

Cisplatin, LY379268, and (S)−3,4-DCPG were purchased from Abcam. Meclizine, HC 030031, AMG 333, NF 110, and AMG 9810 were purchased from Tocris. Cisplatin stocks were dissolved in 1-methyl-2-pyrrolidinone at 8 mg/ml (Sigma-Aldrich). LY379268, (S)−3,4-DCPG, and NF 110 stocks were dissolved in water. Meclizine stocks were dissolved in DMSO. HC 030031, AMG 333, and AMG 9810 were suspended at 50 μM in water employing repeated vortexing and freeze-thaw cycles as necessary until no pellets could be observed after centrifuging at 18,000 rcf. Aliquots of all drugs except cisplatin were stored at −80°C until use. Cisplatin stock was kept at −20°C until use. All drugs were added to 0.9% saline immediately before injection, intraperitoneally. Meclizine was added to water immediately before injection, intraperitoneally. On days that both behavioral testing and injection occurred, animals were weighed before behavioral testing. Mouse weights were used to calculate drug dosage. Injections were performed after behavioral testing. For drugs used in imaging experiments, aliquots from 50 μM stock were vortexed vigorously and diluted to 10 μM final concentration in PBS. Isoflurane was purchased from the Piramal Group (Mumbai, India). Pentobarbital was purchased from Diamondback Drugs. Cisplatin and saline vehicle injections were performed on days 1, 3, 5, and 7. In experiments using multiple rounds of cisplatin injection, cisplatin was also injected on days 12, 14, 16, and 18. When (S)−3,4-DCPG or LY379268 were concomitantly administered to animals receiving cisplatin, injections were given 30 min before cisplatin. When meclizine was concomitantly administered with cisplatin, injections were given 3 h before cisplatin. In imaging experiments where drugs were applied directly to the DRG, the order of drug administration was HC 030031, AMG 333, NF 110, and AMG 9810.

Behavioral tests

von Frey mechanical test

Mice were placed in a 4.5 × 5 × 10 cm transparent container on a metal mesh and allowed to habituate for at least 30 min before testing. Each mouse was tested at a specific force eight times to determine the lowest force required to elicit a paw withdrawal response more than 50% of the time.

Hot plate thermal test

Mice were placed in a 4.5 × 5 × 10 cm transparent container on a temperature controlled hot plate set to 45°C. Latency to acute nocifensive behavior was determined by onset of hindpaw lifts, licking, jumping, or flinching.

DRG exposure surgery

L5 DRG exposure surgery and imaging was performed as previously described (Kim et al., 2016). Mice were anesthetized with pentobarbital (40–50 mg/kg). After deep anesthesia was achieved, the animal's back was shaved, and the shaved skin was aseptically prepared by cleaning with alcohol and iodine pad, and ophthalmic ointment was applied to keep the eyes moist (Lacrilube, Allergan Pharmaceuticals). Mice were kept on a heating pad and monitored with a rectal thermometer to maintain body temperature at 37 ± 0.5°C.

Dorsal laminectomy was performed in the L4–L6 area. A 2-cm midline incision was made in the lower back around the lumbar enlargement area. Paravertebral muscles were dissected away to expose the lower lumbar enlargement area, and the bones were cleaned. Small rongeurs were used to remove the surface aspect of the L5 DRG transverse process bone near the vertebra to expose the DRG without disrupting the neurons, axons, and other cells in the DRG.

In vivo DRG GCaMP Ca^{2+} imaging

In vivo GCaMP Ca^{2+} imaging of the large DRG was performed over 1–6 h following exposure surgery on day 8 after the last of four drug injections on days 1, 3, 5, and 7. Mice were kept on a heating pad and monitored with a rectal thermometer to maintain body temperature at 37 ± 0.5°C. Mice were laid abdomen down on a custom-designed imaging stage. Movement from breathing, heart beats, etc., was minimized by holding the head in a custom designed holder with an anesthesia/gas mask and custom designed vertebral clamps. Continuous anesthesia was maintained with 1−2% isoflurane in pure oxygen.

For imaging and analysis, the stage was fixed under a single photon confocal microscope (Carl Zeiss AG). Raw image stacks (512 × 512–1024 × 1024 pixels in the *x-y* plane and 20- to 30-µm voxel depth) were converted into time lapse movies (~6.5–7 s were required to produce a single frame) and analyzed using Zeiss Zen 3.1 Blue Edition software (Carl Zeiss AG).

Putative responding cells were identified by visual observation of raw image time lapse movies. Ca^{2+} transient intensities were calculated by $\Delta F/F_0 = (F_t - F_0)/F_0$, where F_t is the pixel intensity in a region of interest (Cioroiu and Weimer) at the time point of interest, and F_0 is the baseline intensity determined by averaging the intensities of the first two to six frames of the ROI in the experiment. For calcium responses to stimuli that produced multiple transients, only the first peak was analyzed. Cells showing calcium transients before the stimulus were assumed to be spontaneously active and were not included in analysis of stimuli-induced transients. Each peak of spontaneous Ca^{2+} transients was analyzed individually. Suitable transients (not too much movement of images, clear baseline fluorescence, no nearby cells with Ca^{2+} transients) were randomly sampled for analysis. An effort was made to sample the same number of cells from each DRG for calculating average and SEM for area under the curve (AUC) and $\Delta F/F_0$ intensity; no more than 40% of cells came from a single DRG.

Stimuli were applied carefully so as to not cause movement during imaging. Brush stimuli were applied by repeated gentle brushing from heel to toes approximately once per second using small (5 mm) and large (40 mm) brush bristles. Press (SMALGO Algometer, Bioseb Instruments) and von Frey filaments were applied directly to the hindpaw ipsilateral to the DRG being imaged for 15–20 s. Thermal stimuli were applied by immersing the hindpaw in water at a specific temperature (0°C or 45°C) for 15–20 s. Stimuli were applied after 35–40 s of baseline imaging. HC 030031, AMG 333, NF 110, and AMG 9810 were applied during imaging by topically pipetting onto DRG neurons and allowed to sit for at least 5 min. Between drug applications, neurons were rinsed three to four times in PBS, and the final wash was allowed to sit on the DRG for at least 5 min.

Statistical analysis

Statistics were performed on GraphPad Prism 9.0.1. Ca^{2+} transient intensities and numbers of activated cells showing spontaneous Ca^{2+} activity or Ca^{2+} activity following stimuli were analyzed by Student's *t* test or one-way or two-way ANOVA followed by *post hoc* Tukey's test or *post hoc* Dunnett's test, as appropriate. Specific statistical tests performed are indicated in the text of the results and figure and table legends.

Results

Cisplatin induces mechanical and thermal hyperalgesia, increases spontaneous Ca^{2+} activity in the DRG neurons, and increases the sensitization of DRG neurons to mechanical and thermal stimuli

To determine the effects of cisplatin on DRG Ca^{2+} signaling, animals were injected with cisplatin (3.5 mg/kg, i.p.) every other day for four total injections (Deng et al., 2012). Compared with saline-treated controls, cisplatin-injected animals developed mechanical hyperalgesia after the second injection of cisplatin (Fig. 1*A*, Movie 1; drug effect $F_{(1,48)} = 475.7$, $p < 0.001$; time effect $F_{(3,48)} = 34.4$, $p < 0.001$; interaction $F_{(3,48)} = 40.43$, $p < 0.001$; $n = 7$ per group; Tukey's df = 48, day 4 q = 17.52, $p < 0.001$; day 8 q = 20.88, $p < 0.001$; day 11 q = 21.12, $p < 0.001$) and thermal hyperalgesia after the fourth cisplatin injection (Fig. 1*B*; drug effect $F_{(1,48)} = 35.32$, $p < 0.001$; time effect $F_{(3,48)} = 15.69$, $p < 0.001$; interaction $F_{(3,48)} = 5.378$, $p = 0.0028$; $n = 7$ per group; Tukey's df = 48, day 8 q = 6.722, $p = 0.0005$; day 11 q = 6.974, $p = 0.0003$). Ca^{2+} imaging experiments were performed as previously described (Kim et al., 2016). Animals were anesthetized and DRGs were surgically exposed and imaged. In cisplatin-injected mice, we found significant increases in the numbers of cells with spontaneous Ca^{2+} oscillation ($t_{(18)} = 5.150$, $p = 0.000067$, $n = 11$ saline and 9 cisplatin) and in total spontaneous Ca^{2+} activity (total of spontaneous Ca^{2+} oscillation and steady-state high Ca^{2+} levels; $t_{(18)} = 4.380$, $p = 0.000361$, $n = 11$ saline and 9 cisplatin) compared with saline-injected mice, but no significant increase in the number of cells exhibiting steady-state high Ca^{2+} activity compared with saline-injected mice ($t_{(18)} = 1.800$, $p = 0.088631$, $n = 11$ saline and 9 cisplatin; Fig. 1*C*, Movie 2), indicating that the increase was primarily because of spontaneous Ca^{2+} oscillation. The numbers of DRG neurons responding to press (100, 300, and 600 g), 10-g von Frey, and 45°C stimuli were increased compared with saline controls (Figs. 1*D*, 2*D*, 2*G*, Movie 1; 100 g $t_{(15)} = 3.457$, $p = 0.003523$, $n = 8$ saline and 9 cisplatin; 300 g $t_{(6)} = 3.179$, $p = 0.01910$, $n = 4$ each; 600 g $t_{(6)} = 2.945$, $p = 0.02{,}577$, $n = 4$ each; 10 g $t_{(18)} = 2.386$, $p = 0.02{,}825$, $n = 11$ saline and 9 cisplatin; 45°C $t_{(15)} = 4.625$, $p = 0.000330$, $n = 11$ saline and 9 cisplatin).

Stimulus-induced Ca^{2+} transients were monitored in saline-treated and cisplatin-treated animals. The numbers of cells showing spontaneous Ca^{2+} activity and Ca^{2+} transients in response to stimuli were higher in DRGs of cisplatin-treated animals than in DRGs of saline-treated animals ($F_{(1,47)} = 49.21$, $p < 0.001$ by two-way ANOVA). Average AUC of Ca^{2+} transients of cisplatin group was decreased by a large number of low-amplitude Ca^{2+} transients (many neurons are activated; Fig. 4*C*). Analysis of spontaneous and press-induced Ca^{2+} transients showed that

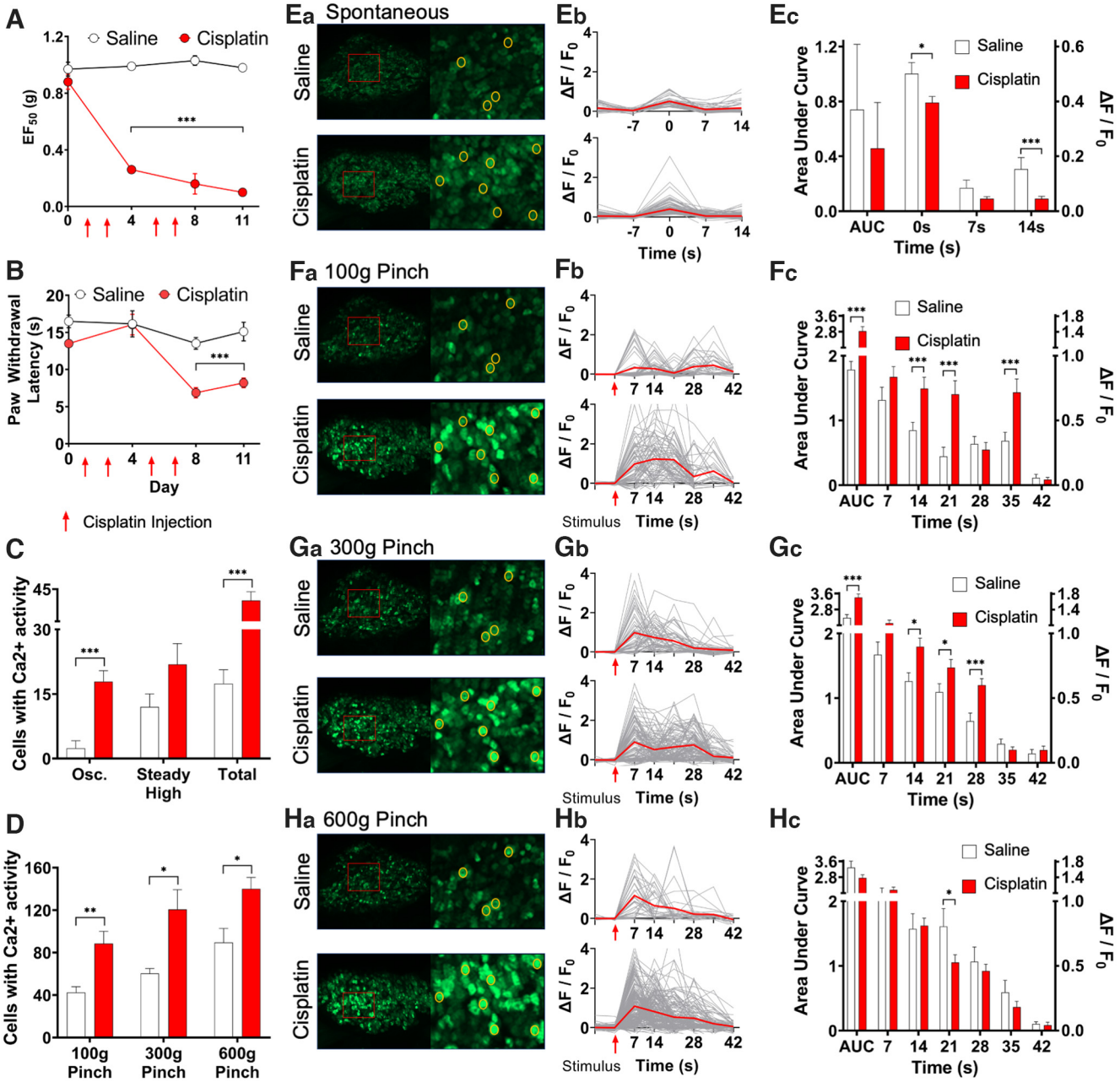

Figure 1. Cisplatin treatment causes increased sensitivity to pain, increases the number of DRG neurons showing Ca^{2+} activity spontaneously or in response to press stimuli and alters Ca^{2+} transient fluorescence intensities and areas under the curve to press stimuli. ***A***, Mechanical pain sensitivity tests using von Frey filaments were performed on days 0, 4, 8, and 11. Red arrows indicate saline or cisplatin injection (days 1, 3, 5, and 7). Mechanical sensitivity is plotted as the 50% withdrawal threshold in grams. ***B***, Thermal pain sensitivity tests using the hot plate assay were performed on days 0, 4, 8, and 11. Arrows indicate day of cisplatin or vehicle (saline) injection (days 1, 3, 5, and 7). Thermal sensitivity is plotted as paw withdrawal latency in seconds. ***C***, DRGs were imaged for spontaneous Ca^{2+} activity following injection of cisplatin or saline in the absence of stimuli. Graphs show number of cells with Ca^{2+} oscillation, steady-state high Ca^{2+}, and total number of cells with Ca^{2+} activity. ***D***, DRGs were imaged during paw press at forces of 100, 300, and 600 g. Graphs show cells producing Ca^{2+} transients in response to press stimuli. ***Ea***, Representative maximum intensity Z-projection images of spontaneous DRG neuronal Ca^{2+} activity in saline-injected and cisplatin-injected animals. Imaged DRGs are shown on left. Area outlined by red boxes are magnified on the right. Yellow circles in ***Ea***, ***Fa***, ***Ga***, ***Ha*** indicate Ca^{2+} activity of neurons in response to different stimuli. ***Eb***, Graphs of spontaneous DRG neuronal Ca^{2+} transients shown with maximum fluorescence intensity set at 0 s. *Y*-axis is expressed as $\Delta F/F_0$ fluorescence intensity. Saline $n = 5$ DRGs, 28 cells, 85 transient peaks. Cisplatin $n = 5$ DRGs, 90 cells, 189 transient peaks. ***Ec***, Mean $\Delta F/F_0$ fluorescence intensities of spontaneous Ca^{2+} transients shown as a function of time. Left *y*-axis, AUC; arbitrary units. Right *y*-axis, $\Delta F/F_0$ fluorescence intensity. ***Fa***, ***Ga***, ***Ha***, Representative maximum intensity Z-projection images of Ca^{2+} activity in response to 100-g (***Fa***), 300-g (***Ga***), or 600-g (***Ha***) press stimulus among DRG neurons in saline-injected and cisplatin-injected animals. All panels (and subpanels) ***E***–***H*** are sequentially derived from a single DRG neuronal ensemble from either a saline-injected animal or a cisplatin-injected animal. Areas outlined by red boxes are magnified on the right. ***Fb***, ***Gb***, ***Hb***, Graphs of Ca^{2+} transients in response to press stimuli. Arrow indicates start of press stimulus. *Y*-axis, $\Delta F/F_0$ fluorescence intensity. Saline, $n = 3$, 3, and 3 DRGs; $n = 88$, 105, and 48 cells for 100, 300, and 600 g, respectively. Cisplatin $n = 3$, 3, and 3 DRGs; $n = 51$, 189, and 186 cells for 100, 300, and 600 g, respectively. ***Fc***, ***Gc***, ***Hc***, Mean fluorescence intensities of Ca^{2+} transients in response to press stimuli. Left *y*-axis, AUC; arbitrary units. Right *y*-axis, $\Delta F/F_0$ fluorescence intensity for each frame. All graphs with error bars show mean ± SEM. Transient plots show all individual analyzed cells in gray lines and mean $\Delta F/F_0$ in red. For behavior, animal numbers are saline, $n = 14$ (8 males, 6 females), cisplatin, $n = 13$ (8 males, 5 females). Numbers of DRGs analyzed for spontaneous activity, 100-, 300-, and 600-g press were saline, $n = 11$, 8, 4, and 4, respectively, cisplatin, $n = 9$, 9, 4, and 4, respectively. Please see further detail in Tables 1-3 and in Figure 4*C*. Comparisons of numbers of cells showing Ca^{2+} transients were performed using Student's *t* test. Comparisons of fluorescence intensities of Ca^{2+} transients were performed with two-way ANOVA followed by Tukey's *post hoc* tests; saline versus cisplatin $^*p < 0.05$, $^{**}p < 0.01$, $^{***}p < 0.001$.

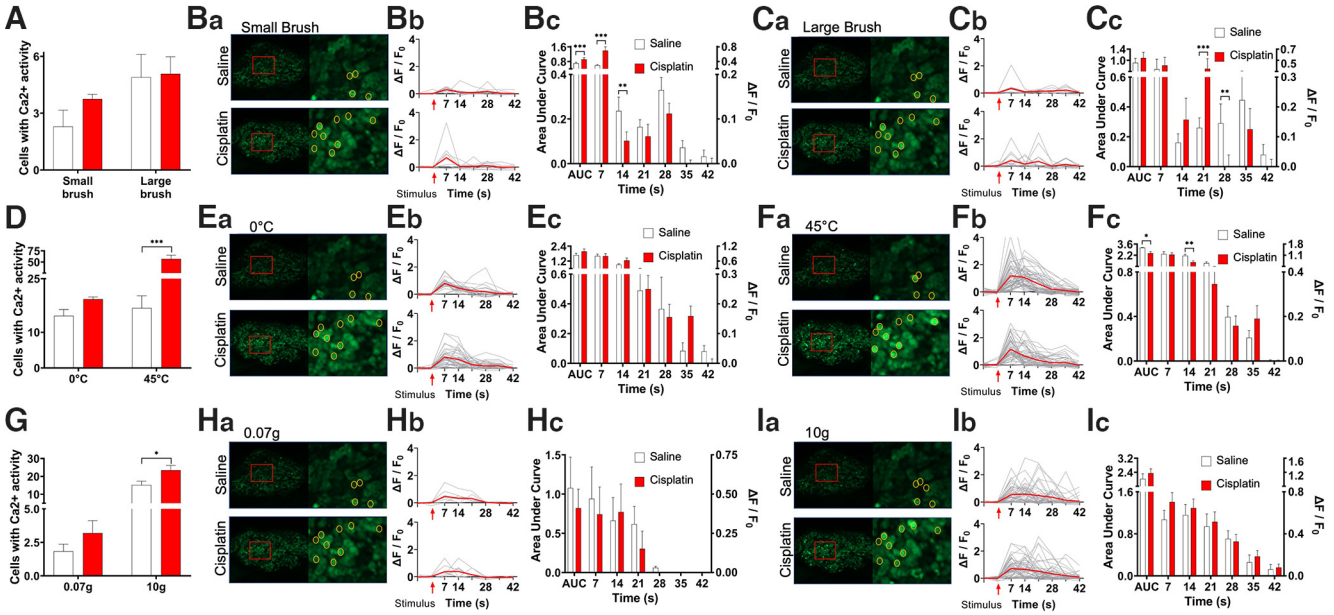

Figure 2. Cisplatin treatment increases the number of Ca^{2+}-activated DRG neurons responding to thermal and strong von Frey stimuli and alters Ca^{2+} transient fluorescence intensities and AUC in response to thermal stimuli. ***A***, ***D***, ***G***, DRGs were imaged during stimulation using small brush and large brush (***A***), paw immersion in 0°C and 45°C water (***D***), and 0.07- and 10-g von Frey filaments (***G***). Graphs show cells producing Ca^{2+} transients in response to different stimuli. ***Ba***, ***Ca***, ***Ea***, ***Fa***, ***Ha***, ***Ia***, Representative images (maximum intensity Z-projections from saline-injected and cisplatin-injected animals) of DRG neuronal Ca^{2+} activity in response to stimuli: small brush (***Ba***), large brush (***Ca***), 0°C cold (***Ea***), 45°C hot (***Fa***), 0.07-g von Frey (***Ha***), and 10-g von Frey (***Ia***). All panels (and subpanels) ***B***, ***C***, ***E***, ***F***, ***H***, ***I*** are sequentially derived from a single DRG neuronal ensemble from either a saline-injected animal or a cisplatin-injected animal. Areas outlined by red boxes are magnified on the right. Yellow circles track Ca^{2+} activity of two sets of DRG neurons (in saline-injected mice vs cisplatin-injected mice) through different stimuli. ***Bb***, ***Cb***, ***Eb***, ***Fb***, ***Hb***, ***Ib***, Graphs of Ca^{2+} transients in response to various stimuli. Arrow indicates start of stimulus. *Y*-axis, $\Delta F/F_0$ fluorescence intensity. ***Bc***, ***Cc***, ***Ec***, ***Fc***, ***Hc***, ***Ic***, Mean fluorescence intensities of Ca^{2+} transients in response to various stimuli. Left *y*-axis, AUC; arbitrary units. Right *y*-axis, $\Delta F/F_0$ fluorescence intensity for each frame. Numbers of DRGs analyzed for cell counts for small brush, large brush, 0°C water, 45°C water, 0.07-g von Frey, and 10-g von Frey were: saline, $n = 7$, 6, 5, 9, 6, and 11, respectively; cisplatin, $n = 4$, 5, 4, 8, 5, and 9, respectively. Numbers of cells analyzed for Ca^{2+} transients for small brush, large brush, 0°C water, 45°C water, 0.07-g von Frey, and 10-g von Frey were: saline, $n = 10$, 11, 27, 61, 7, and 45, respectively; cisplatin, $n = 10$, 16, 40, 51, 8, and 55, respectively. Please see further detail in Tables 2 and 3 and in Figure 4*C*. All graphs with error bars show mean ± SEM. Transient plots show all individual analyzed cells in gray lines and mean $\Delta F/F_0$ in red. Comparisons of numbers of cells showing Ca^{2+} transients were performed using Student's *t* test. Comparisons of fluorescence intensities of Ca^{2+} transients were performed with two-way ANOVA followed by Tukey's *post hoc* tests; saline versus cisplatin $^*p < 0.05$, $^{**}p < 0.01$, $^{***}p < 0.001$.

spontaneous Ca^{2+} transients in the DRG of saline-treated controls took longer to return to baseline than in cisplatin-treated animals (Fig. 1*Eb*,*Ec*; drug effect $F_{(1,684)} = 17.38$, $p < 0.001$; time effect $F_{(2,684)} = 147.6$, $p < 0.001$; interaction $F_{(2,684)} = 1.207$, $p = 0.2997$; $n = 43$ saline, 189 cisplatin; Tukey's df = 684, 0 s q = 4.256, $p = 0.0323$; 7 s q = 1.621, $p = 0.8617$; 14 s q = 6.263, $p = 0.0002$). At 100- and 300-g press, cisplatin-treated animals had greater AUC and were slower to return to baseline than saline-treated animals (Fig. 1*Fb*,*Fc*,*Gb*,*Gc*; 100 g, AUC $t_{(233)} = 3.533$, $p = 0.000499$; drug effect $F_{(1,1068)} = 16.88$, $p < 0.001$; time effect $F_{(5,1068)} = 13.33$, $p < 0.001$; interaction $F_{(5,1068)} = 2.788$, $p = 0.0165$; $n = 88$ saline, 137 cisplatin; Tukey's df = 1068, 7 s q = 2.276, $p = 0.9057$; 14 s q = 6.274, $p = 0.0006$; 21 s q = 7.668, $p < 0.0001$; 28 s q = 0.5069, $p > 0.9999$; 35 s q = 6.544, $p = 0.0003$; 300 g, AUC $t_{(292)} = 3.878$, $p = 0.000130$; drug effect $F_{(1,1554)} = 15.04$, $p = 0.001$; time effect $F_{(5,1554)} = 48.06$, $p < 0.001$; interaction $F_{(5,1554)} = 1.779$, $p = 0.1140$; $n = 105$ saline, 189 cisplatin; Tukey's df = 1554, 7 s q = 3.724, $p = 0.2619$; 14 s q = 5.281, $p = 0.0105$; 21 s q = 4.777, $p = 0.0360$; 28 s q = 6.345, p 0.0005). Ca^{2+} transients at 600-g press were not significantly different between saline-treated and cisplatin-treated animals (Fig. 1*H*; drug effect $F_{(1,1073)} = 1.277$, $p = 0.2587$; time effect $F_{(5,1073)} = 29.62$, $p < 0.0001$; interaction $F_{(5,1073)} = 1.066$, $p = 0.3774$). Compared with Ca^{2+} transients in DRG neurons of saline-treated mice, cisplatin treatment increased AUC of Ca^{2+} transients in response to small brush stimulus and decreased AUC of Ca^{2+} transients in response to paw immersion in 45°C water (Fig. 2*Bb*,*Bc*,*Fb*,*Fc*; small brush AUC $t_{(18)} = 6.069$, $p = 0.00001$; drug effect $F_{(1,104)} = 23.54$, $p < 0.0001$; time effect $F_{(5,104)} = 498.9$, $p < 0.0001$; interaction $F_{(5,104)} = 123.8$, $p < 0.0001$; $n = 10$ saline, 10 cisplatin; Tukey's df = 104, 7 s q = 34.87, $p < 0.0001$; 14 s q = 5.798, $p = 0.0045$; 45°C drug effect $F_{(1,623)} = 5.675$, $p = 0.0175$; time effect $F_{(5,623)} = 62.38$, $p < 0.0001$; interaction $F_{(5,623)} = 2.559$, $p = 0.0264$; $n = 61$ saline, 51 cisplatin; Tukey's df = 623, 7 s q = 0.511, $p > 0.9999$; 14 s q = 5.185, $p = 0.0141$). Compared with saline-treated controls, more Ca^{2+} transients were delayed in cisplatin-treated animals in response to large brush stimulus (Fig. 2*Cc*; drug effect $F_{(1,136)} = 0.5561$, $p = 0.4571$; time effect $F_{(5,136)} = 37.74$, $p < 0.0001$; interaction $F_{(5,136)} = 10.31$, $p < 0.0001$; $n = 11$ saline, 16 cisplatin; Tukey's df = 136, 7 s q = 2.479, $p = 0.8400$; 14 s q = 2.726, $p = 0.7398$; 21 s q = 7.500, $p < 0.0001$; 28 s q = 5.980, $p = 0.0024$; 35 s q = 3.181, $p = 0.5175$). Amplitude of Ca^{2+} transients in response to paw immersion in 45°C water was significantly higher in saline-treated animals than in cisplatin-treated animals (Fig. 2*Fc*; AUC $t_{(110)} = 2.568$, $p = 0.01156$; drug effect $F_{(1,623)} = 5.675$, $p = 0.0175$; time effect $F_{(5,623)} = 62.38$, $p < 0.0001$; interaction $F_{(5,623)} = 2.559$, $p = 0.0264$; $n = 61$ saline, 51 cisplatin; Tukey's df = 623, 7 s q = 0.5110, $p > 0.9999$; 14 s q = 5.815, $p = 0.0141$; 21 s q = 3.223, $p = 0.4928$; 28 s q = 0.4958, $p > 0.9999$; 35 s q = 0.9730, $p > 0.9999$). Paw immersion in 0°C water, or paw stimulus with 0.07- and 10-g von Frey, did not show significant differences between Ca^{2+} transients of two groups (Fig. 2*Eb*,*Ec*,*Hb*,*Hc*,*Ib*,*Ic*; drug effect 0°C $F_{(1,364)} = 0.9285$, $p = 0.3359$; 0.07 g $F_{(1,73)} = 0.3066$, $p = 0.5815$; 10 g $F_{(1,525)} = 1.199$, $p = 0.2740$).

Table 1. Comparisons of cell diameter of DRG neurons responding to press stimuli in saline-treated controls and cisplatin-treated animals

Press responses		
Diameter	Saline	Cisplatin
100-g pinch: number of activated cells (proportion of activated cells)		
Small (<20 μm)	22.00 ± 4.51, $n = 3$ (55.9 ± 8.4%)	46.33 ± 7.75, $n = 3$ (67.6 ± 3.8%)
Medium (20–25 μm)	12.67 ± 3.53, $n = 3$ (33.6 ± 8.7%)	17.67 ± 2.40, $n = 3$ (25.2 ± 0.2%)
Large (>25 μm)	4.00 ± 0.58, $n = 3$ (10.5 ± 2.0%)	4.33 ± 2.19, $n = 3$ (7.2 ± 3.7%)
300-g pinch: number of activated cells (proportion of activated cells)		
Small	40.33 ± 5.90, $n = 3$ (53.4 ± 6.7%)	52.00 ± 12.12, $n = 3$ (51.9 ± 12.7%)
Medium	23.67 ± 2.03, $n = 3$ (31.6 ± 3.4%)	29.67 ± 6.12, $n = 3$ (29.4 ± 18.7%)
Large	11.33 ± 2.33, $n = 3$ (15.0 ± 3.6%)	19.00 ± 8.62, $n = 3$ (18.7 ± 7.9%)
600-g pinch: number of activated cells (proportion of activated cells)		
Small	49.00 ± 15.72, $n = 3$ (51.2 ± 7.5%)	64.00 ± 7.77, $n = 3$ (49.5 ± 5.6%)
Medium	26.33 ± 2.96, $n = 3$ (31.4 ± 5.6%)	41.67 ± 2.03, $n = 3$ (32.0 ± 2.1%)
Large	15.00 ± 2.52, $n = 3$ (17.4 ± 3.1%)	23.67 ± 5.36, $n = 3$ (18.4 ± 4.3%)

Most activated neurons were small (<20 μm) or medium (20–25 μm) diameter. Strong mechanical stimuli (300- and 600-g press) activated a higher proportion of large diameter (>25 μm) neurons. Proportions of small versus medium versus large diameter neurons were not statistically distinguishable between groups. *N*, numbers of DRGs analyzed for cell diameter.

Table 2. Comparisons of cell diameter of DRG neurons responding to different stimuli in saline-treated controls and cisplatin-treated, cisplatin plus (S)−3,4-DCPG-treated, and cisplatin plus meclizine-treated animals.

Spontaneous and stimulus responses following pharmacological treatment				
Diameter	Saline	Cisplatin	Cisplatin + DCPG	Cisplatin + meclizine
Spontaneous Ca^{2+} activation				
Small	3.80 ± 1.20, n =s 5	13.17 ± 2.77, $n = 6$	15.67 ± 13.67, $n = 3$	5.40 ± 1.60, $n = 5$
Medium	1.80 ± 0.58, $n = 5$	2.67 ± 0.67, $n = 6$	1.33 ± 0.88, $n = 3$	2.20 ± 1.32, $n = 5$
Large	0.00 ± 0.00, $n = 5$	1.67 ± 0.71, $n = 6$	0.00 ± 0.00, $n = 3$	0.80 ± 0.58, $n = 5$
0°C cold				
Small	12.67 ± 2.73, $n = 3$	17.33 ± 1.20, $n = 3$	29.33 ± 1.20, $n = 3$	10.33 ± 4.84, $n = 3$
Medium	1.33 ± 0.33, $n = 3$	1.33 ± 1.33, $n = 3$	3.67 ± 1.45, $n = 3$	2.33 ± 0.88, $n = 3$
Large	0 ± 0.00, $n = 3$	0 ± 0.00, $n = 3$	1.00 ± 0.58, $n = 3$	0.00 ± 0.00, $n = 3$
45°C hot				
Small	18.67 ± 2.03, $n = 3$	34.33 ± 10.33, $n = 3$	29.00 ± 7.23, $n = 3$	17.33 ± 3.84, $n = 3$
Medium	6.33 ± 0.88, $n = 3$	10.33 ± 0.33, $n = 3$	5.33 ± 1.20, $n = 3$	3.67 ± 1.86, $n = 3$
Large	0 ± 0.00, $n = 3$	0 ± 0.00, $n = 3$	0.33 ± 0.33, $n = 3$	0.33 ± 0.33, $n = 3$
0.07-g von Frey				
Small	1 ± 0.00, $n = 3$	3.33 ± 0.33, $n = 3$	1.8 ± 0.58, $n = 5$	3.00 ± 2.52, $n = 3$
Medium	1.33 ± 0.67, $n = 3$	0.33 ± 0.33, $n = 3$	0.2 ± 0.20, $n = 5$	0.33 ± 0.33, $n = 3$
Large	0 ± 0.00, $n = 3$	0 ± 0.00, $n = 3$	0 ± 0.00, $n = 5$	0.33 ± 0.33, $n = 3$
10-g von Frey				
Small	3.67 ± 2.33, $n = 3$	11 ± 3.06, $n = 3$	22.67 ± 7.31, $n = 3$	11.33 ± 4.41, $n = 3$
Medium	8.33 ± 4.37, $n = 3$	7.67 ± 1.33, $n = 3$	6.00 ± 1.53, $n = 3$	6.33 ± 2.19, $n = 3$
Large	4.00 ± 2.08, $n = 3$	2.67 ± 1.76, $n = 3$	5.00 ± 1.15, $n = 3$	3.67 ± 1.45, $n = 3$

Most activated neurons were small (<20 μm) or medium (20–25 μm) diameter. Strong mechanical stimulus (10-g von Frey) tended to activate a higher proportion of large diameter (>25 μm) neurons. *N*, number of DRGs analyzed for cell diameter.

The relative proportions of small, medium, and large diameter neurons that exhibited spontaneous Ca^{2+} oscillation and response to stimuli were indistinguishable between cisplatin-treated and saline-treated mice. Nonetheless, following cell activation, spontaneous Ca^{2+} transients and Ca^{2+} transients following most stimuli predominantly occurred in small diameter neurons (<20 μm), followed by medium diameter neurons (20–25 μm), and finally, relatively few large diameter neurons (>25 μm). However, more large diameter neurons were activated by stronger mechanical stimuli (10-g von Frey, 300- and 600-g press) than by other stimuli, albeit still a lower proportion than small and medium diameter neurons (Tables 1, 2).

Cisplatin-induced hyperalgesia is attenuated by concomitant administration of mGluR8 agonist, (S)−3,4-DCPG

Since mGluR8 agonists are known to attenuate some kinds of inflammatory pain (Marabese et al., 2007; Palazzo et al., 2011), we tested mGluR8 agonist, (S)−3,4-DCPG, in the cisplatin-induced pain model by injecting (S)−3,4-DCPG (30 mg/kg, i.p.) 30 min before each cisplatin injection. (S)−3,4-DCPG attenuated cisplatin-induced mechanical and thermal hyperalgesia (Fig. 3*A*, *B*; mechanical drug effect $F_{(2,221)} = 463.7$, $p < 0.0001$; time effect $F_{(12,221)} = 6.148$, $p < 0.0001$; interaction $F_{(24,221)} = 3.563$, $p < 0.001$; $n = 7$ saline, 7 cisplatin, 6 cisplatin plus (S)−3,4-DCPG; Tukey's df = 221 cisplatin vs cisplatin plus (S)−3,4-DCPG df = 221, day 0 q = 1.120, $p = 0.7085$; day 4 q = 1.120, $p < 0.0001$; cisplatin vs saline day 0 q = 1.311, $p = 0.6238$, day 4 q = 10.63, $p < 0.0001$; thermal drug effect $F_{(2,234)} = 40.91$, $p < 0.0001$; time effect $F_{(12,234)} = 8.010$, $p < 0.001$; interaction $F_{(24,234)} = 2.424$, $p = 0.0004$; $n = 6$ saline, 6 cisplatin, 9 cisplatin + (S)−3,4-DCPG; Tukey's cisplatin vs cisplatin plus (S)−3,4-DCPG df = 234, day 0 q = 1.007, $p = 0.7566$; day 8 q = 4.964, $p = 0.0016$). However, neither the number of activated neurons showing spontaneous Ca^{2+} activity nor the number of activated neurons responding to 45°C, 0.07-g von Frey, 10-g von Frey, or 100-g press stimuli were

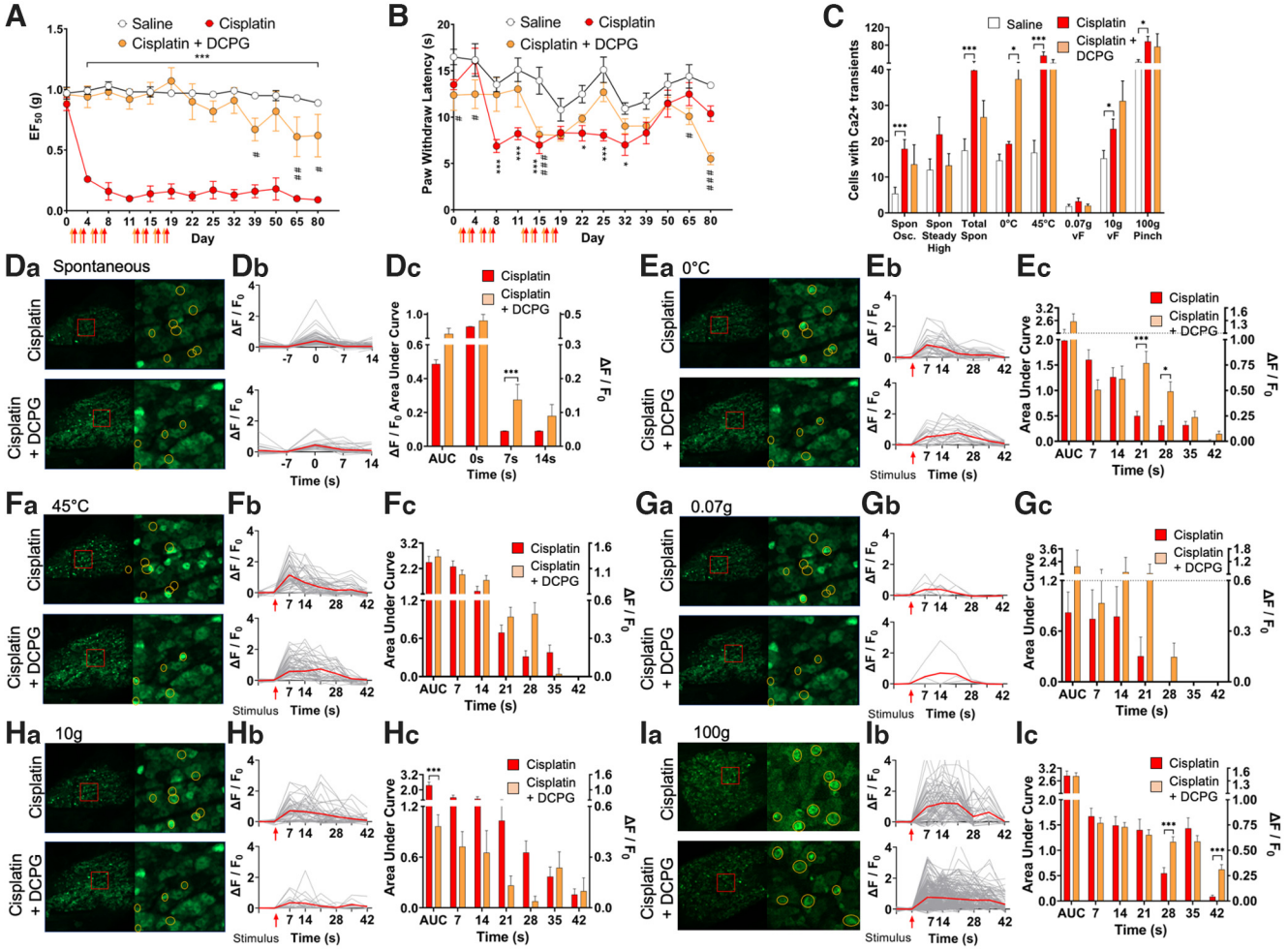

Figure 3. mGluR 8 agonist, (S)−3,4-DCPG reduces mechanical and thermal pain sensitivity in cisplatin-treated animals and affects Ca^{2+} activity in response to some stimuli. ***A***, Mechanical pain sensitivity tests using von Frey filaments were performed every 3–15 d up to 80 d. Red arrows indicate injection of saline or cisplatin (days 1, 3, 5, 7, 12, 14, 16, 18); orange arrows indicate injection of (S)−3,4-DCPG or saline vehicle 30 min before cisplatin injection. Mechanical sensitivity is plotted as 50% withdrawal threshold (grams). Saline $n = 7$ (5 males, 2 females), cisplatin $n = 7$ (5 males, 2 females), cisplatin + (***S***)−3,4-DCPG $n = 6$ (3 males, 3 females). ***B***, Thermal pain sensitivity tests using hot plate assay were performed every 3–15 d up to 80 d. Red arrows indicate injection of saline or cisplatin (days 1, 3, 5, 7, 12, 14, 16, 18); orange arrows indicate injection of (S)−3,4-DCPG or saline vehicle 30 min before cisplatin injection. Thermal sensitivity is plotted as paw withdrawal latency in seconds. Animal numbers are the same as in panel ***A***. ***C***, DRGs were imaged for spontaneous Ca^{2+} activity in the absence of stimuli and during stimulation of the hindpaw with 0°C, 45°C, 0.07-g von Frey, 10-g von Frey, and 100-g press. Graphs show numbers of cells producing Ca^{2+} transients spontaneously, steady-state high cytosol Ca^{2+}, total spontaneous activity, and in response to stimuli. ***Da***, Representative images (maximum intensity Z-projections) of spontaneous DRG neuronal Ca^{2+} activity in cisplatin-injected or cisplatin plus (S)−3,4-DCPG-injected animals. Imaged DRGs are shown on left. Areas outlined by red boxes are magnified on the right. Yellow circles track Ca^{2+} activity of two sets of DRG neurons (in cisplatin-injected mice versus cisplatin plus (S)−3,4-DCPG-injected mice) through different stimuli (in later panels). ***Db***, Graphs of spontaneous DRG neuronal Ca^{2+} transients are shown with maximum fluorescence intensity set at 0 s. *Y*-axis, $\Delta F/F_0$ fluorescence intensity. Cisplatin, $n = 5$ DRGs, 90 cells, 189 transient peaks. (S)−3,4-DCPG, $n = 4$ DRGs, 37 cells, 83 transient peaks. ***Dc***, Mean fluorescence intensities of spontaneous DRG neuronal Ca^{2+} transients as a function of time. Left *y*-axis, AUC, arbitrary units. Right *y*-axis, $\Delta F/F_0$ fluorescence intensity. ***Ea***, ***Fa***, ***Ga***, ***Ha***, ***Ia***, Representative images (maximum intensity Z-projections) of Ca^{2+} transients in response to different stimuli: 0°C cold (***Ea***), 45°C hot (***Fa***), 0.07-g von Frey (***Ga***), 10-g von Frey (***Ha***), and 100-g press (***Ia***) of cisplatin-injected and cisplatin plus (S)−3,4-DCPG-injected animals. Areas outlined by red boxes are magnified on the right. Yellow circles permit comparison of DRG neurons activated by different stimuli. ***Eb***, ***Fb***, ***Gb***, ***Hb***, ***Ib***, Graphs of DRG neuronal Ca^{2+} transients in response to different stimuli: 0°C cold (***Eb***), 45°C hot (***Fb***), 0.07-g von Frey (***Gb***),10-g von Frey, and 100-g press (***Ib***). Red arrow indicates start of each stimulus. *Y*-axis, $\Delta F/F_0$ fluorescence intensity. ***Ec***, ***Fc***, ***Gc***, ***Hc***, ***Ic***, Mean fluorescence intensities of DRG neuronal Ca^{2+} transients in response to various stimuli. Left *y*-axis, AUC, arbitrary units. Right *y*-axis, $\Delta F/F_0$ fluorescence intensity. All panels (and subpanels) ***D***, ***E***, ***F***, ***G***, ***H*** (except ***I***) are sequentially derived from a single DRG neuronal ensemble from either a cisplatin -injected animal or a cisplatin plus (S)−3,4-DCPG-injected animal. Transient plots show all individually analyzed cells in gray lines and mean $\Delta F/F_0$ in red. Numbers of DRGs analyzed for 0°C water, 45°C water, 0.07-g von Frey, 10-g von Frey, and 100-g press were, respectively: saline, $n = 5$, 9, 6, 11, and 8; cisplatin, $n = 4$, 8, 5, 9 and 9; cisplatin plus (S)−3,4-DCPG, $n = 5$, 4, 3, 4, and 4. Numbers of cells analyzed for transients for 0°C water, 45°C water, 0.07-g von Frey, 10-g von Frey, and 100-g press were, respectively: cisplatin, $n = 40$, 51, 8, 55, and 137 and (S)−3,4-DCPG, $n = 25$, 40, 4, 20, and 243. Please see further detail in Tables 2 and 3 and in Figure 4*C*. All graphs with error bars show mean ± SEM. Behavioral, AUC, and transient intensity comparisons were performed using two-way ANOVA followed by Tukey's *post hoc* tests. Cell count comparisons of saline-injected and (S)−3,4-DCPG plus cisplatin-injected versus cisplatin-injected animals were performed by one-way ANOVA followed by Dunnett's *post hoc* test; for behavioral comparisons: saline versus cisplatin and cisplatin versus cisplatin + (S)−3,4-DCPG $^*p < 0.05$, $^{**}p < 0.01$, $^{***}p < 0.001$; saline versus cisplatin $\#p < 0.05$, $\#\#p < 0.01$, $\#\#\#p < 0.001$, for cell counts and Ca^{2+} transients $^*p < 0.05$, $^{**}p < 0.01$, $^{***}p < 0.001$.

different between cisplatin-treated and cisplatin plus (S)−3,4-DCPG-treated animals (Fig. 3*C*; 45°C $t_{(16)} = 1.448$, $p = 0.1696$, $n = 8$ each; 0.07 g $t_{(8)} = 1.177$, $p = 0.2731$, $n = 5$ each; 10 g $t_{(15)} = 1.305$, $p = 0.2114$, $n = 9$ cisplatin, 8 cisplatin plus (S)−3,4-DCPG; 100 g $t_{(11)} = 0.4550$, $p = 0.6580$, $n = 9$ cisplatin, 4 cisplatin + (S)−3,4-DCPG). The number of activated neurons following 0°C cold stimulus was increased in cisplatin plus (S)−3,4-DCPG animals compared with cisplatin-only controls (Fig. 3*C*; $t_{(5)} = 4.845$, $p = 0.04903$, $n = 4$ cisplatin, 3 cisplatin plus (S)−3,4-DCPG). (S)−3,4-DCPG slowed spontaneous decay

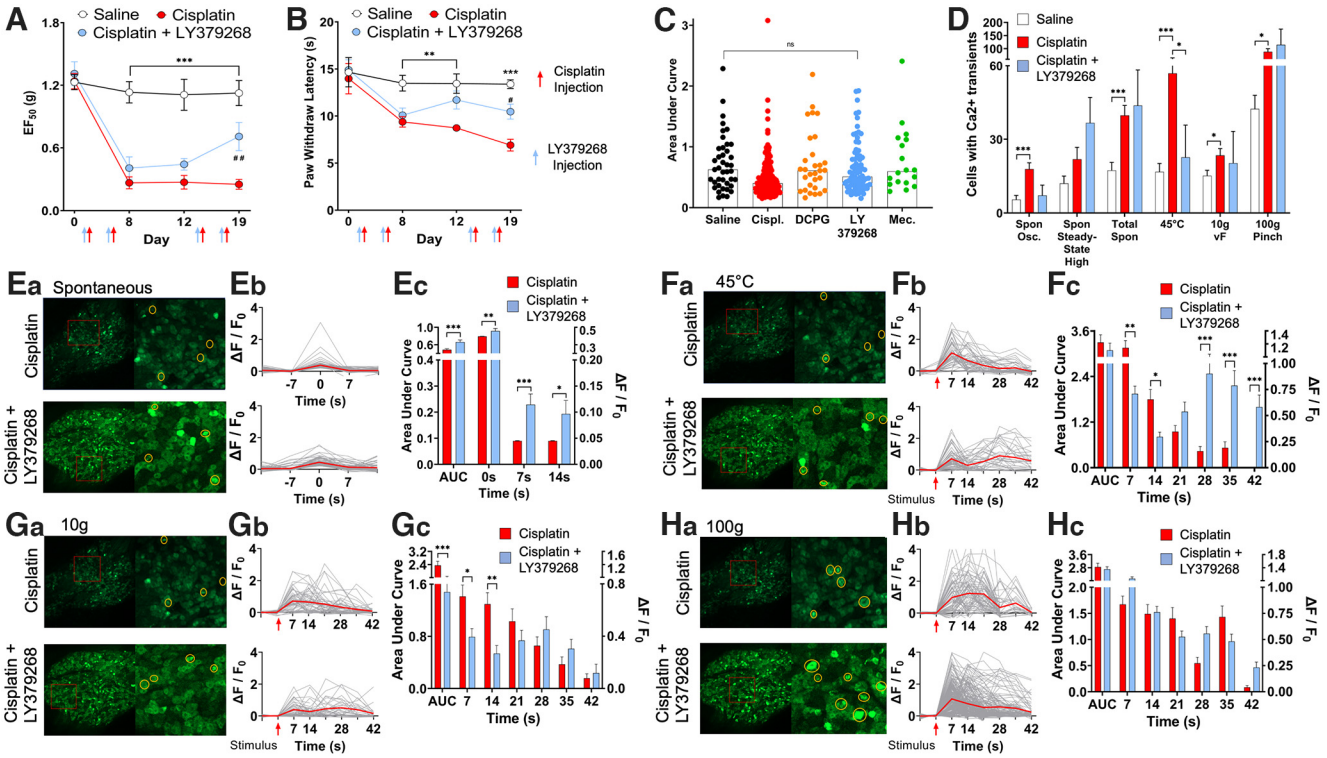

Figure 4. mGluRs 2/3 agonist, LY379268, reduces mechanical and thermal pain sensitivity in cisplatin-treated animals and reduces DRG neuronal Ca^{2+} activity in response to thermal stimulus. ***A***, ***B***, Mechanical pain sensitivity tests using von Frey filaments and thermal pain sensitivity tests using hot plate were performed before injection and on days 8, 12, and 19 following the start of injections. Red arrows indicate injection of cisplatin (days 3, 5, 14, 16). Blue arrows indicate injection of LY379268 30 min before cisplatin injection. Mechanical sensitivity is plotted as 50% withdrawal threshold (grams). Thermal sensitivity is plotted as paw withdrawal latency (seconds). Numbers of animals were: saline, $n = 12$ (6 males, 6 females); cisplatin, $n = 12$ (6 males, 6 females); LY379268, $n = 7$ (3 males, 4 females). ***C***, AUC of Ca^{2+} transients of individual spontaneous oscillating neurons. Groups are saline controls, cisplatin, cisplatin plus DCPG, cisplatin plus LY379268, and cisplatin plus meclizine. AUCs are shown. Except panel ***C***, graphs show mean ± SEM. ***D***, DRGs were imaged for spontaneous Ca^{2+} activity in the absence of stimuli and during stimulation of the hindpaw with 45°C, 10-g von Frey, and 100-g press. Graphs show numbers of cells producing Ca^{2+} transients spontaneously, steady-state high cytosol Ca^{2+}, total spontaneous Ca^{2+} activity, and activity in response to stimuli. ***Ea***, Representative images (maximum intensity Z-projections) of spontaneous DRG neuronal Ca^{2+} activity in cisplatin-injected, or cisplatin plus LY379268-injected animals. Imaged DRGs are shown on left. Areas outlined by red boxes are magnified on the right. Yellow circles indicate spontaneous Ca^{2+} activity and Ca^{2+} activity following various stimuli in later panels. ***Eb***, Graphs of spontaneous DRG neuronal Ca^{2+} transients are shown with the first frame of fluorescence intensity increase set at 0 s. *Y*-axis, $\Delta F/F_0$ fluorescence intensity. Cisplatin, $n = 5$ DRGs, 90 cells, 189 transient peaks. LY379268, $n = 3$ DRGs, 21 cells, 51 transient peaks. ***Ec***, Mean fluorescence intensities of spontaneous DRG neuronal Ca^{2+} transients as a function of time frame. Left *y*-axis, AUC, arbitrary units. Right *y*-axis, $\Delta F/F_0$ fluorescence intensity. ***Fa***, ***Ga***, ***Ha***, Representative images (maximum intensity Z-projections) of Ca^{2+} transients in response to different stimuli: 45°C hot (***Fb***), 10-g von Frey (***Gb***), and 100-g press (***Hb***) of cisplatin-injected and cisplatin plus LY379268-injected animals. Areas outlined by red boxes are magnified on the right. Yellow circles indicate DRG neurons activated by different stimuli. ***Fb***, ***Gb***, ***Hb***, Graphs of DRG neuronal Ca^{2+} transients in response to different stimuli: 45°C hot (***Fb***), 10-g von Frey (***Gb***), and 100-g press (***Hb***). Red arrow indicates start of each stimulus. *Y*-axis, $\Delta F/F_0$ fluorescence intensity. ***Fc***, ***Gc***, ***Hc***, Mean fluorescence intensities of DRG neuronal Ca^{2+} transients in response to various stimuli. Left *y*-axis, AUC, arbitrary units. Right *y*-axis, $\Delta F/F_0$ fluorescence intensity. All graphs with error bars show mean ± SEM. Transient plots show all individually analyzed cells in gray lines and mean $\Delta F/F_0$ in red. Numbers of DRGs analyzed for 45°C water, 10-g von Frey, and 100-g press were, respectively: saline, $n = 9$, 11, and 8: cisplatin, $n = 8$, 9, and 9; cisplatin plus LY379268, $n = 3$, 3, and 3. Numbers of cells analyzed for 45°C water, 10-g von Frey, and 100-g press were, respectively: cisplatin, $n = 51$, 55, and 137 and LY379268, $n = 66$, 51, and 255. Please see further detail in Tables 2 and 3. Behavioral, AUC, and Ca^{2+} transient intensity comparisons of saline-injected and LY379268 plus cisplatin-injected animals versus cisplatin-injected animals are two-way ANOVA followed by Dunnett's *post hoc* test. Cell count comparisons of saline-injected and LY379268 plus cisplatin-injected versus cisplatin-injected animals were performed by one-way ANOVA followed by Dunnett's *post hoc* test. For behavioral tests: saline versus cisplatin $^*p < 0.05$, $^{**}p < 0.01$, $^{***}p < 0.001$; cisplatin versus cisplatin plus LY379268 $\#p < 0.05$, $\#\#p < 0.01$, $\#\#\#p < 0.001$, for cell counts and Ca^{2+} transients: cisplatin versus cisplatin plus LY379268 $^*p < 0.05$, $^{**}p < 0.01$, $^{***}p < 0.001$.

time of Ca^{2+} transients (return to baseline; Fig. 3*Db*,*Dc*; drug effect $F_{(1,655)} = 34.58$, $p < 0.001$; time effect $F_{(2,684)} = 454.8$, $p < 0.001$; interaction $F_{(2,684)} = 1.987$, $p = 0.1379$; $n = 189$ cisplatin, 33 (S)−3,4-DCPG + cisplatin; Tukey's df = 655, 0 s q = 3.889, $p = 0.0671$; 7 s q = 7.092, $p < 0.001$; 14 s q = 3.425, $p = 0.1502$). (S)−3,4-DCPG also increased the neuronal number of delayed Ca^{2+} transients in response to 0°C cold (Fig. 3*Eb*,*Ec*; drug effect $F_{(1,366)} = 6.630$, $p = 0.0104$; time effect $F_{(5,366)} = 20.26$, $p < 0.001$; interaction $F_{(5,366)} = 6.794$, $p < 0.001$; $n = 40$ cisplatin, 25 cisplatin plus (S)−3,4-DCPG; Tukey's df = 366, 7 s q = 3.887, $p = 0.2072$; 14 s q = 0.2487, $p > 0.9999$; 21 s q = 6.720, $p = 0.0002$; 28 s q = 4.831, $p = 0.0338$) but decreased AUC of Ca^{2+} transients in response to 10-g von Frey stimulus (Fig. 3*Hb*,*Hc*; $t_{(73)} = 3.469$, $p = 0.000879$, $n = 55$ cisplatin, 20 cisplatin plus (S)−3,4-DCPG).

Cisplatin-induced hyperalgesia and the numbers of spontaneous Ca^{2+}-activated cells are attenuated by Group II mGluR agonist, LY379268

Group II mGluRs are strong candidate analgesic targets for inflammatory pain (Mazzitelli et al., 2018). We tested effects of the mGlu2/3 receptor agonist, LY379268, on cisplatin-induced pain in the cisplatin-induced animal model. We found that injection of LY379268 (10 mg/kg, i.p.) 30 min before each cisplatin injection reduced cisplatin-induced mechanical and thermal hyperalgesia by day 19 (Fig. 4*A*,*B*; mechanical drug effect $F_{(2,109)} = 60.27$, $p < 0.0001$; time effect $F_{(3,109)} = 38.62$, $p < 0.0001$; interaction $F_{(6,109)} = 8.617$, $p < 0.0001$; $n = 12$ saline, 12 cisplatin, 7 cisplatin plus LY379268; Dunnett's df = 109, cisplatin vs cisplatin plus LY379268, day 0 q = 0.5559, $p = 0.8075$; day 8 q = 1.149, $p = 0.4264$; day 12 q = 1.380, $p = 0.3016$; day 19

q = 3.404, $p = 0.0019$; cisplatin vs saline, df = 109 d 0 q = 0.08549, $p = 0.9949$; day 8 q = 8.339, $p < 0.0001$; day 12 q = 6.727, $p < 0.0001$; day 19 q = 6.847, $p < 0.0001$; thermal drug effect $F_{(2,67)} = 17.68$, $p < 0.0001$; time effect $F_{(3,67)} = 11.57$, $p < 0.0001$; interaction $F_{(6,67)} = 1.889$, $p = 0.0955$; $n = 7$ per group; Dunnett's cisplatin vs cisplatin plus LY379268, df = 67, day 0 q = 0.6970, $p = 0.7072$; day 8 q = 0.5504, $p = 0.8049$; day 12 q = 2.213, $p = 0.0550$; day 19 q = 2.551, $p = 0.0244$; cisplatin vs saline, df = 67, day 0 q = 0.4930, $p = 0.8378$; day 8 q = 3.180, $p = 0.0043$; day 12 q = 3.507, $p = 0.0016$; day 19 q = 4.819, $p < 0.0001$). The numbers of activated neurons following 45°C hot stimulus was decreased in cisplatin plus LY379268-treated animals compared with cisplatin-treated controls (Fig. 4*D*; $t_{(9)} = 2.279$, $p = 0.04868$, $n = 8$ cisplatin, 3 cisplatin plus LY379268). LY379268 increased AUC and slowed decay time of spontaneous Ca^{2+} transients (Fig. 4*Ec*; AUC $t_{(264)} = 3.641$, $p = 0.000327$, $n = 189$ cisplatin, 77 cisplatin plus LY379268 drug effect $F_{(1,783)} = 40.79$, $p < 0.0001$; time effect $F_{(2,783)} = 609.2$, $p < 0.0001$; interaction $F_{(2,783)} = 0.2899$, $p = 0.7484$; Tukey's df = 783 0 s q = 3.767, $p = 0.0005$; 7 s q = 4.234, $p < 0.0001$; 14 s q = 2.684, $p = 0.0221$) Spontaneous amplitude was not statistically distinguishable from saline (Dunnett's saline vs cisplatin plus LY379268 df = 340 q = 0.8542 $p > 0.999$). LY379268 slowed decay time of Ca^{2+} transients following 45°C (Fig. 4*Fc*; drug effect $F_{(1,543)} = 20.27$, $p < 0.0001$; time effect $F_{(5,543)} = 14.28$, $p < 0.0001$; interaction $F_{(5,543)} = 19.43$, $p < 0.0001$; $n = 51$ cisplatin, 66 cisplatin plus LY379268; Tukey's df = 543 7 s q = 5.766, $p = 0.0030$; 14 s q = 4.781, $p = 0.0369$; 21 s q = 2.2800, $p = 0.9042$; 28 s q = 8.299, $p < 0.0001$; 35 s q = 6.328, $p = 0.0006$; 42 s q = 6.198, $p = 0.0009$).

Cisplatin-induced mechanical hyperalgesia, spontaneous DRG neuronal Ca^{2+} activity, and Ca^{2+} response to 45°C hot stimulus are attenuated by histamine receptor 1 antagonist, meclizine

Since meclizine has a protective role against DNA damage by cisplatin (Gorgun et al., 2017), we tested meclizine in cisplatin-treated animals for its effects on behavior and Ca^{2+} activity. Meclizine was injected (16 mg/kg, i.p.) 3 h before cisplatin injection (3.5 mg/kg, i.p.) four times over 8 d. Meclizine reduced cisplatin-induced mechanical hypersensitivity (Fig. 5*A*; drug effect $F_{(2,129)} = 45.55$, $p < 0.0001$; time effect $F_{(3,109)} = 27.65$, $p < 0.0001$; interaction $F_{(6,109)} = 5.729$, $p < 0.0001$; $n = 12$ saline, 15 cisplatin, 16 cisplatin plus meclizine; Dunnett's cisplatin vs cisplatin plus meclizine, df = 129 d 0 q = 0.004792, $p > 0.9999$; day 8 q = 3.078, $p = 0.0050$; day 12 q = 3.052, $p = 0.0054$; day 19 q = 2.958, $p = 0.0073$; cisplatin vs saline, df = 129 d 0 q = 0.07429, $p = 0.9960$; day 8 q = 7.246, $p < 0.0001$; day 12 q = 5.845, $p < 0.0001$; day 19 q = 5.949, $p < 0.0001$) and reduced cisplatin-induced thermal hypersensitivity (Fig. 5*B*; drug effect $F_{(2,63)} = 19.04$, $p < 0.0001$; time effect $F_{(3,63)} = 7.403$, $p = 0.0003$; interaction $F_{(6,63)} = 2.958$, $p = 0.0131$; $n = 7$ saline, 7 cisplatin, 6 cisplatin plus meclizine; Dunnett's cisplatin vs cisplatin plus meclizine, df = 63 d 0 q = 0.004792, $p > 0.9999$; day 8 q = 3.078, $p = 0.0050$; day 12 q = 3.052, $p = 0.0054$; day 19 q = 2.958, $p = 0.0073$; cisplatin vs saline, df = 129 d 0 q = 0.07429, $p = 0.9960$; day 8 q = 7.246, $p < 0.0001$; day 12 q = 5.845, $p < 0.0001$; day 19 q = 5.949, $p < 0.0001$). Meclizine also attenuated spontaneous Ca^{2+} activity in cisplatin-treated animals, reducing the numbers of neurons exhibiting spontaneous Ca^{2+} activity (Ca^{2+} oscillation plus steady-state high Ca^{2+}) down to numbers comparable to numbers seen in saline-treated animals (Fig. 5*C*,*D*; oscillation $t_{(15)} = 2.872$, $p = 0.01163$, $n = 9$ cisplatin, 8 cisplatin plus meclizine; steady high $t_{(14)} = 2.134$, $p = 0.05098$, $n = 9$ cisplatin, 7 cisplatin plus meclizine; total spontaneous activity $t_{(14)} = 4.112$, $p = 0.01056$, $n = 9$ cisplatin, 7 cisplatin plus meclizine), and reduced the numbers of Ca^{2+}-activated neurons in response to 100-g press (mechanical stimulus) and 45°C water (thermal stimulus; Fig. 5*C*,*Da*, Movie 3; 100 g $t_{(14)} = 2.197$, $p = 0.04532$, $n = 9$ cisplatin, 7 cisplatin plus meclizine; 45°C $t_{(15)} = 3.500$, $p = 0.00322$, $n = 9$ cisplatin, 8 cisplatin plus meclizine). In addition, meclizine treatment significantly increased the AUC of Ca^{2+} transients and decay time (return to baseline) in response to 0°C water (cold stimulus; Fig. 5*Eb*,*Ec*; 0°C AUC $t_{(87)} = 2.187$, $p = 0.03146$, drug effect $F_{(1,505)} = 9.078$, $p = 0.0027$; time effect $F_{(5,505)} = 35.90$, $p < 0.0001$; interaction $F_{(5,505)} = 7.338$, $p < 0.0001$; $n = 40$ cisplatin, 49 cisplatin plus meclizine; Tukey's df = 505 7 s q = 4.679, $p = 0.0463$; 14 s q = 1.973, $p = 0.9642$; 21 s q = 6.654, $p = 0.0002$; 28 s q = 4.284, $p = 0.1032$; 35 s q = 1.589, $p = 0.9935$; 42 s q = 0.5821, $p > 0.9999$). In contrast, meclizine reduced AUC of Ca^{2+} transients in response to 45°C water (Fig. 5*Fb*,*Fc*; AUC $t_{(59)} = 2.519$, $p = 0.01451$, drug effect $F_{(1,501)} = 0.3214$, $p = 0.5710$; time effect $F_{(5,501)} = 45.65$, $p < 0.0001$; interaction $F_{(5,501)} = 0.1126$, $p = 0.1126$; $n = 40$ cisplatin, 21 cisplatin plus meclizine; Tukey's df = 501 7 s q = 5.132, $p = 0.0163$; 14 s q = 1.513, $p = 0.9958$; 21 s q = 0.7778, $p > 0.9999$; 28 s q = 0.07723, $p > 0.9999$; 35 s q = 2.394, $p = 0.8709$; 42 s q = 0.0000, $p > 0.9999$), 10-g von Frey (Fig. 5*Hb*,*Hc*; 10 g AUC $t_{(80)} = 3.580$, $p = 0.000587$, drug effect $F_{(1,424)} = 12.13$, $p = 0.0005$; time effect $F_{(5,424)} = 8.542$, $p < 0.0001$; interaction $F_{(5,424)} = 2.385$, $p = 0.0376$; $n = 55$ cisplatin, 27 cisplatin plus meclizine; Tukey's df = 424 7 s q = 5.415, $p = 0.0081$; 14 s q = 1.739, $p = 0.9864$, 21 s q = 4.117, $p = 0.1406$, 28 s q = 2.583, $p = 0.8026$, 35 s q = 1.523, $p = 0.9955$, 42 s q = 1.019, $p = 0.9999$), and 100-g press (Fig. 5*Ib*,*Ic*; AUC $t_{(257)} = 4.063$, $p = 0.000065$, drug effect $F_{(1,1089)} = 33.17$, $p < 0.0001$; time effect $F_{(5,1089)} = 9.116$, $p < 0.0001$; interaction $F_{(5,1089)} = 4.919$, $p = 0.0001$; $n = 137$ cisplatin, 122 cisplatin plus meclizine; Tukey's df = 1089 7 s q = 8.499, $p < 0.0001$; 14 s q = 5.082, $p = 0.0176$, 21 s q = 4.6700, $p = 0.0460$, 28 s q = 0.5574, $p > 0.9999$, 35 s q = 5.8300, $p = 0.0024$, 42 s q = 0.1629, $p > 0.9999$). Meclizine caused no detectable change on Ca^{2+} transients in response to 0.07-g von Frey ($p > 0.5$; Fig. 5*Gb*,*Gc*; drug effect $F_{(1,85)} = 0.08211$, $p = 0.7752$; time effect $F_{(5,85)} = 6.552$, $p < 0.0001$; interaction $F_{(5,85)} = 0.9157$, $p = 0.4749$; $n = 8$ cisplatin, 10 cisplatin plus meclizine).

Cisplatin-induced weight loss is attenuated by meclizine and LY379268 but unaffected by (S)−3,4-DCPG

Cachexia, a condition associated with cancer and characterized by weight loss, muscle loss, and adipose loss, increases cancer mortality (Fearon et al., 2013), and is exacerbated by nearly every form of chemotherapy (Langer et al., 2002; Kazemi-Bajestani et al., 2016). Here, we monitored cisplatin-associated weight loss over the time course of experiments. Cisplatin treatment was associated with rapid, persistent weight loss (Fig. 6*A*–*C*). Concomitant (S)−3,4-DCPG treatment had no attenuating effect on weight loss (Fig. 6*A*). Cisplatin-associated body weight loss among (S)−3,4-DCPG-treated animals returned to baseline levels 32 d after the last cisplatin injection (Fig. 6*A*; Dunnett's df = 425 cisplatin vs cisplatin plus (S)−3,4-DCPG day 58 q = 1.020, $p = 0.4924$). Animals that received concomitant LY379268 experienced less weight loss over the course of injections than cisplatin-treated controls (Fig. 6*B*; drug effect $F_{(2,191)} = 124.9$, $p < 0.0001$; time effect $F_{(10,191)} = 25.30$, $p < 0.0001$; interaction $F_{(20,191)} = 3.375$, $p < 0.0001$; $n = 7$ each, Dunnett's df = 191 cisplatin vs cisplatin plus LY379268 day 18 q = 2.294, $p = 0.421$). Animals that received concomitant meclizine administration experienced moderate weight loss (drug

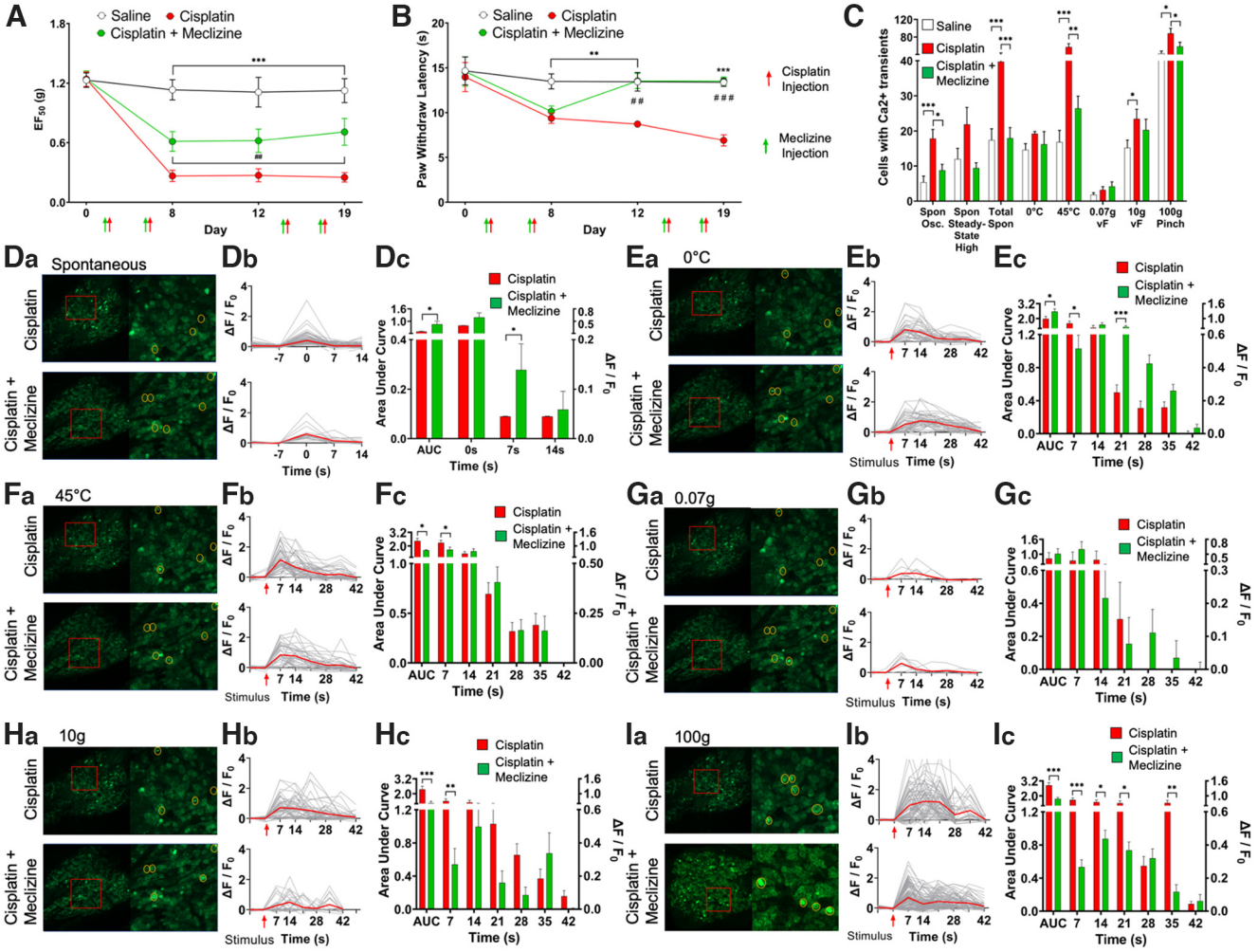

Figure 5. Meclizine attenuates cisplatin-induced mechanical and thermal pain sensitivity and reduces spontaneous DRG neuronal Ca^{2+} activity and Ca^{2+} activity in response to thermal and mechanical stimuli. ***A***, ***B***, Graphs show mechanical and thermal pain sensitivity tests using von Frey filaments or 45°C hot plate before injection and on days 8, 12, and 19 following the start of injections. Red arrows indicate saline or cisplatin injection, and green arrows indicate meclizine or vehicle injection 3 h before cisplatin injection (days 3, 5, 14, 16). Mechanical sensitivity is plotted as 50% withdrawal threshold in grams. Thermal sensitivity is plotted as paw withdrawal latency (seconds). Saline, $n = 14$ (8 males, 6 females); cisplatin, $n = 13$ (8 males, 5 females); meclizine, $n = 12$ (6 males, 6 females), days 1, 8, 12, and $n = 6$ (3 males, 3 females) day 19. ***C***, DRGs were imaged for spontaneous Ca^{2+} activity in the absence of stimuli and during stimulation of the hindpaw with 0°C, 45°C, 0.07g von Frey, 10g von Frey, and 100g press. Graphs show numbers of cells producing Ca^{2+} transients spontaneously , steady-state high cytosol Ca^{2+}, total spontaneous Ca^{2+} activity, and activity in response to stimuli. ***Da***, Representative images of spontaneous DRG neuronal Ca^{2+} activity in cisplatin-injected, or cisplatin plus meclizine-injected animals. Imaged DRGs are shown on left. Areas outlined by red boxes are magnified on the right. Yellow circles indicate spontaneously activating neurons. ***Db***, Graphs of spontaneous DRG neuronal Ca^{2+} transients are shown, maximum fluorescence intensity set at 0 s. *Y*-axis, $\Delta F/F_0$ fluorescence intensity. Cisplatin, $n = 5$ DRGs, 90 cells, 189 transient peaks. Meclizine $n = 4$ DRGs, 24 cells, 30 transient peaks. ***Dc***, Mean fluorescence intensities of spontaneous Ca^{2+} transients as a function of time frame. Left *y*-axis, AUC, arbitrary units. Right *y*-axis, $\Delta F/F_0$ fluorescence intensity. ***Ea***, ***Fa***, ***Ga***, ***Ha***, ***Ia***, Representative images of DRG neuronal Ca^{2+} activity in response to stimuli: 0°C cold (***Ea***), 45° C hot (***Fa***), 0.07-g von Frey (***Ga***), 10-g von Frey (***Ha***), and 100-g press (***Ia***) of cisplatin-injected and cisplatin plus meclizine-injected animals. Areas outlined by red boxes are magnified on the right. Yellow circles indicate Ca^{2+} activating neurons with different stimuli. ***Eb***, ***Fb***, ***Gb***, ***Hb***, ***Ib***, Graphs of DRG neuronal Ca^{2+} transients in response to various stimuli. Red arrow indicates start of each stimulus. *Y*-axis, $\Delta F/F_0$ fluorescence intensity. ***Ec***, ***Fc***, ***Gc***, ***Hc***, ***Ic***, Mean fluorescence intensities of DRG neuronal Ca^{2+} transients in response to various stimuli. Left *y*-axis, AUC, arbitrary units. Right *y*-axis, $\Delta F/F_0$ fluorescence intensity. All graphs with error bars show mean ± SEM. Transient plots show all individually analyzed cells in gray lines and mean $\Delta F/F_0$ in red. Numbers of DRGs analyzed for 0°C water, 45°C water, 0.07-g von Frey, 10-g von Frey, and 100-g press were, respectively: saline, $n = 5$, 9, 6, 11, and 8; cisplatin, $n = 4$, 8, 5, 9, and 9; cisplatin plus meclizine, $n = 5$, 4, 9, 7, and 4. Numbers of cells analyzed for transients for 0°C water, 45°C water, 0.07-g von Frey, 10-g von Frey, and 100-g press were, respectively: cisplatin, $n = 40$, 51, 8, 55, and 137 and meclizine, $n = 49$, 40, 10, 27, and 122. Please see further detail in Tables 2 and 3 and Figure 4*C*. Behavioral comparisons of saline-injected and meclizine plus cisplatin-injected versus cisplatin-injected animals are two-way ANOVA followed by Dunnett's *post hoc* test. AUC and transient intensity comparisons are two-way ANOVA followed by Tukey's test. Cell count comparisons of saline-injected and meclizine plus cisplatin-injected versus cisplatin-injected animals were performed by one-way ANOVA followed by Dunnett's *post hoc* test. For behavioral tests: saline versus cisplatin, $*p < 0.05$, $**p < 0.01$, $***p < 0.001$; cisplatin versus cisplatin plus meclizine, $\#p < 0.05$, $\#\#p < 0.01$, $\#\#\#p < 0.001$. For cell counts and Ca^{2+} transients: cisplatin versus cisplatin plus meclizine $*p < 0.05$, $**p < 0.01$, $***p < 0.001$.

effect $F_{(2,154)} = 50.01$, $p < 0.0001$; time effect $F_{(10,154)} = 3.595$, $p = 0.0003$; interaction $F_{(20,154)} = 1.753$, $p = 0.0306$; $n = 7$ saline, 7 cisplatin, 6 cisplatin plus meclizine) and returned to baseline within 10 d after the fourth injection. We also observed a late effect, as body weight of meclizine-treated animals began decreasing 50 d after the last injection (Fig. 6*C*; Dunnett's df = 191 cisplatin vs cisplatin plus meclizine day 18 q = 1.385, $p = 0.2922$).

TRP channel inhibitors administered directly onto DRGs during imaging experiments reduces the number of cells producing spontaneous Ca^{2+} transients and NF 110 and AMG 9810 sensitize saline-treated animals to 45°C stimulus

In order to study somatosensory ion channels or receptors involved in cisplatin-induced drug hypersensitivity, we applied four TRP channel inhibitors to DRG to study their effects on spontaneous activity and four stimuli: large brush, 10-g von

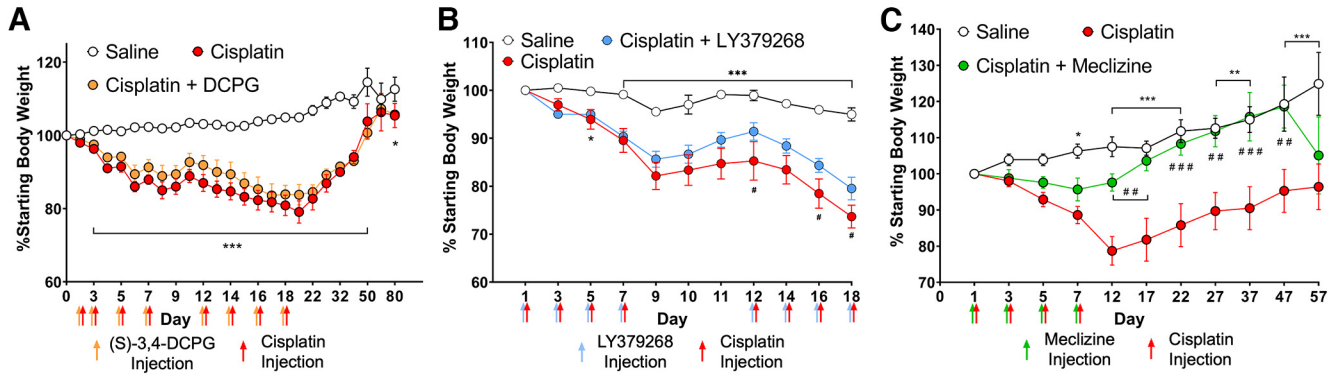

Figure 6. Cisplatin treatment results in significant body weight loss in mice which is attenuated by meclizine and LY379268 treatment but not by (S)−3,4-DCPG treatment. ***A***, Changes in body weight over the course of mechanical and thermal sensitivity experiments using animals injected with saline, cisplatin, or cisplatin plus (S)−3,4-DCPG (from Fig. 3). *Y*-axis, Percent of starting body weight. Red arrow indicates cisplatin or saline vehicle injection. Orange arrow indicates (S)−3,4-DCPG or saline vehicle injection 30 min before cisplatin injection. Saline, $n = 7$ (5 males, 2 females); cisplatin, $n = 7$ (5 males, 2 females); cisplatin plus (S)−3,4-DCPG, $n = 6$ (3 males, 3 females). ***B***, Changes in body weight over the course of mechanical and thermal sensitivity experiments using animals injected with saline, cisplatin, or cisplatin plus LY379268 (from Fig. 4). Red arrow indicates cisplatin or saline vehicle injection. Blue arrow indicates LY379268 or saline vehicle injection 30 min before cisplatin injection. Saline, $n = 14$ (8 males, 6 females); cisplatin, $n = 13$ (8 males, 5 females); cisplatin plus LY379268, $n = 6$ (3 males, 3 females). ***C***, Changes in body weight over the course of mechanical and thermal sensitivity experiments using animals injected with saline, cisplatin, or cisplatin plus meclizine (from Fig. 5). Red arrow indicates injection of cisplatin or saline vehicle. Green arrow indicates injection of meclizine or saline vehicle 3 h before cisplatin injection. Saline, $n = 6$ (3 males, 3 females); cisplatin, $n = 8$ (5 males, 3 females); cisplatin plus meclizine, $n = 6$ (3 males, 3 females). All graphs show mean ± SEM. Comparisons were performed using two-way ANOVA followed by Dunnett's *post hoc* test. Saline versus cisplatin, $*p < 0.05$, $**p < 0.01$, $***p < 0.001$; cisplatin versus cisplatin plus drug $\#p < 0.05$, $\#\#p < 0.01$, $\#\#\#p < 0.001$.

Table 3. *F* values from two-way ANOVA on the number of cells producing Ca^{2+} transients spontaneously in the absence of stimuli, spontaneous steady-state high cytosol Ca^{2+} activity, total spontaneous Ca^{2+} activity, and response to large brush, 10-g von Frey, 100-g press, and paw immersion in 45°C water before and after application of TRP channel inhibitor

Stimulus	Main baseline and TRP channel inhibitor effect	Main treatment group effect	Interaction
Spontaneous oscillation	$F_{(4,82)} = 4.843$, $p = 0.0015$**	$F_{(4,82)} = 2.667$, $p = 0.0380$*	$F_{(16,82)} = 0.4225$, $p = 0.9725$
Spontaneous steady-state high	$F_{(4,77)} = 0.8213$, $p = 0.5156$	$F_{(4,77)} = 10.60$, $p = 0.001$**	$F_{(16,77)} = 0.1395$, $p > 0.999$
Spontaneous activity, total	$F_{(4,79)} = 1.491$, $p = 0.2129$	$F_{(4,79)} = 9.285$, $p < 0.001$***	$F_{(16,79)} = 0.6552$, $p = 0.8281$
Large brush	$F_{(4,69)} = 1.870$, $p = 0.1255$	$F_{(4,69)} = 0.8954$, $p = 0.4715$	$F_{(16,69)} = 1.114$, $p = 0.3600$
10-g von Frey	$F_{(4,76)} = 1.396$, $p = 0.2436$	$F_{(4,76)} = 2.372$, $p = 0.0597$	$F_{(16,76)} = 0.8977$, $p = 0.5743$
100-g pinch	$F_{(4,67)} = 1.169$, $p = 0.3323$	$F_{(4,67)} = 0.3033$, $p = 0.8748$	$F_{(16,67)} = 0.8516$, $p = 0.6246$
45°C hot	$F_{(4,78)} = 1.590$, $p = 0.1853$	$F_{(4,78)} = 7.194$, $p < 0.001$***	$F_{(16,78)} = 1.395$, $p = 0.1663$

Inhibitors and their targets were HC 030031 (TRPA1), AMG 333 (TRPM8), NF 110 (P2X3 and P2X2/3 heteromultimers), and AMG 9810 (TRPV1). Treatment groups were saline, cisplatin, cisplatin plus LY379268, cisplatin plus (S)−3,4-DCPG, and cisplatin plus meclizine. $*p < 0.05$, $**p < 0.01$, $***p < 0.001$.

Frey, 100-g press, and hindpaw immersion in 45°C water. The TRP channel inhibitors used and their targets were HC 030031 (TRPA1; McNamara et al., 2007), AMG 333 (TRPM8; Horne et al., 2018), NF 110 (P2X3 and P2X2/3 heteromultimers; Hausmann et al., 2006), and AMG 9810 (TRPV1; Doherty et al., 2005).

The number of cells with Ca^{2+} activity in response to stimuli was largely unaffected by inhibitor application. Treatment with inhibitors reduced spontaneous Ca^{2+} transients (drug effect $F_{(4,82)} = 4.843$, $p = 0.0015$) but this effect was indistinguishable between treatment groups (drug x treatment group interaction $F_{(16,82)} = 0.4225$, $p = 0.9725$). The treatment group of the animals was more likely to have an effect on the number of cells with Ca^{2+} activity (for a complete list of *F* and *p* values, see Table 3), but the treatment group was not associated with a significant effect of any TRP channel inhibitor.

Application of NF 110 to DRG had a striking effect on Ca^{2+} transients in response to 45°C (Fig. 7*Ia*,*Ib*,*Ic*; saline controls AUC $t_{(102)} = 3.242$, $p = 0.001607$; inhibitor effect $F_{(1,387)} = 16.17$, $p < 0.001$; time effect $F_{(5,387)} = 4.493$, $p = 0.0005$; interaction $F_{(5,387)} = 2.204$, $p = 0.0532$; $n = 44$ baseline, 60 NF 110; Tukey's df = 387, 7 s q = 0.635, $p > 0.9999$; 14 s q = 7.050, $p < 0.0001$; Cisplatin AUC $t_{(211)} = 4.407$, $p = 0.000017$; inhibitor effect $F_{(1,874)} = 12.62$, $p = 0.0004$; time effect $F_{(5,874)} = 9.165$, $p < 0.0001$; interaction $F_{(5,874)} = 3.070$, $p = 0.0094$; $n = 126$ baseline, 79 NF 110; Tukey's df = 874, 7 s q = 1.079, $p = 0.9998$; 14 s q = 6.297, $p = 0.0006$; 21 s q = 5.469, $p = 0.0066$). No other TRP channel inhibitor had a significant effect on Ca^{2+} transient fluorescence intensity in response to 45°C (data not shown). NF 110 had no detectable effect on Ca^{2+} transient fluorescence intensity in response to mechanical stimuli (data not shown). In addition, in saline-treated animals, NF 110 and AMG 9810 increased the number of cells producing Ca^{2+} transients in response to 45°C, but there were no effects on any other treatment group (Fig. 7*H*; saline $F_{(4,19)} = 4.506$, $p = 0.0099$; *n* = baseline 9, HC 030031 4, AMG 333 4, NF 110 3, AMG 9810 3; Dunnett's df = 18, HC 030031 q = 0.2484, $p = 0.9979$; AMG 333 q = 0.9985, $p = 0.7607$; NF 110 q = 3.060, $p = 0.0238$; AMG 9810 q = 3.329, $p = 0.0132$).

Discussion

CIPN is a painful, debilitating, and complex phenomenon that occurs commonly in patients treated with chemotherapeutic drugs. Various chemotherapeutic drugs act through different molecular and cellular mechanisms, suggesting that causes of CIPN are similarly diverse (Quasthoff and Hartung, 2002; Seretny et al., 2014; Addington and Freimer, 2016; Cioroiu and Weimer, 2017; Flatters et al., 2017). This suggests that the treatment of CIPN should be guided by the chemotherapeutic drug used. The DRG is a site of peripheral sensory neuropathy. Therefore, we sought to study the

Table 4. Numbers of DRGs analyzed for cell counts during TRP channel inhibitor treatment experiments

Stimulus	Saline	Cisplatin	Cisplatin + LY379268	Cisplatin + (S)−3,4-DCPG	Cisplatin + meclizine
Baseline					
Spontaneous activity	11	9	3	9	8
Large brush	10	13	3	4	4
10-g von Frey	11	9	3	8	7
100-g pinch	8	9	3	4	4
45°C hot	9	8	3	8	9
After HC 030031					
Spontaneous activity	4	3	3	3	4
Large brush	3	3	3	3	3
10-g von Frey	4	4	3	3	3
100-g pinch	4	3	3	3	3
45°C hot	4	3	3	3	4
After AMG 333					
Spontaneous activity	4	3	3	3	4
Large brush	3	3	3	3	3
10-g von Frey	4	3	3	3	3
100-g pinch	5	3	3	3	3
45°C hot	5	3	3	3	4
After NF 110					
Spontaneous activity	3	3	3	3	4
Large brush	3	3	3	3	3
10-g von Frey	3	3	3	3	3
100-g pinch	3	4	3	3	3
45°C hot	3	3	3	3	4
After AMG 9810					
Spontaneous activity	3	3	3	3	4
Large brush	3	3	3	3	3
10-g von Frey	3	3	3	3	3
100-g pinch	3	3	3	3	3
45°C hot	3	3	3	3	4

effects of specific chemotherapeutic agents and specific therapies on peripheral neurons and to understand how specific therapies affect responses to different mechanical, thermal, and chemical stimuli. To accomplish this, we used *in vivo* GCaMP Ca^{2+} imaging of the large population of DRG neurons (>1800/DRG), which enabled us to analyze neuronal firing and activity at a population level as an ensemble. Such *in vivo* imaging allows for the detection and study of physiologically important phenomena that would be a challenge to detect using more conventional methods such as electrophysiological recordings (Kim et al., 2016).

Prior research has shown that cisplatin treatment induces spontaneous activity and hyperexcitability in dissociated primary sensory neurons *in vitro* (Laumet et al., 2020). Here, using *in vivo* ensemble analysis of the large array of DRG neurons in an animal model of CIPN, we found that in response to several mechanical and thermal stimuli Ca^{2+} activity and Ca^{2+} transients were increased by cisplatin treatment. The increased numbers of DRG neurons showing Ca^{2+} activity in response to mechanical and thermal stimuli are consistent with mechanical and thermal hypersensitivity observed in behavioral tests. As expected, strong mechanical stimuli caused larger diameter (>25 μm) neurons to activate more often, while thermal, cold, and weak mechanical stimuli (0.07-g von Frey) activated few if any large diameter neurons, consistent with other reports (Kim et al., 2016; Chisholm et al., 2018; Ishida et al., 2021). Previous work has shown activation of increased numbers of DRG neurons in response to stimuli in a variety of pain models (Kim et al., 2016; Chisholm et al., 2018; Kucharczyk et al., 2020; Ishida et al., 2021). Taken together, these results show that the numbers of DRG neurons activated in response to stimuli measured by Pirt-GCaMP3 fluorescence is a valid indicator of peripheral pain hypersensitivity. Our results show that concomitant administration of (S)−3,4-DCPG, LY379268, or meclizine attenuated CIPN mechanical and thermal pain hypersensitivity. Our results also show that two of three drugs (meclizine, LY379268) which attenuated CIPN pain hypersensitivity also attenuated the number of neurons exhibiting spontaneous Ca^{2+} activation. Furthermore, concomitant meclizine or LY379268 administration reduced cisplatin-induced weight loss.

Cisplatin increased the fluorescence intensity of Ca^{2+} transients for several mechanical stimuli (100- or 300-g press or small brush). Interpretation of AUC and plots of fluorescence intensity must be done carefully. Increases in average AUC and amplitude of Ca^{2+} transients should indicate a stronger response to stimuli (e.g., neurons firing more action potentials, upregulation of voltage-gated and other Ca^{2+} channels, lowered thresholds for Ca^{2+} channel activation, increased efflux of Ca^{2+} from ER or mitochondria, etc.). However, these same factors that cause increased numbers of neurons to produce Ca^{2+} transients with higher amplitudes can increase baseline cytosolic Ca^{2+} concentrations and, therefore, increased baseline fluorescence. It is important to note that plots of fluorescence depend on the change in fluorescent intensity relative to baseline. Cisplatin-treated animals generally exhibit higher overall baseline fluorescence intensity (increased F_0). This reduces the $\Delta F/F_0$ ratio, reducing the calculated AUC. Despite the apparently elevated baseline intensities, the calculated AUC in cisplatin-treated animals was nearly always at least as high as in saline vehicle-treated control animals and often higher. An alternative, nonmutually exclusive possibility, is that the increased number of cells producing Ca^{2+} transients in response to cisplatin treatment produce low amplitude transients, which would reduce the average amplitude (Fig. 4*C*).

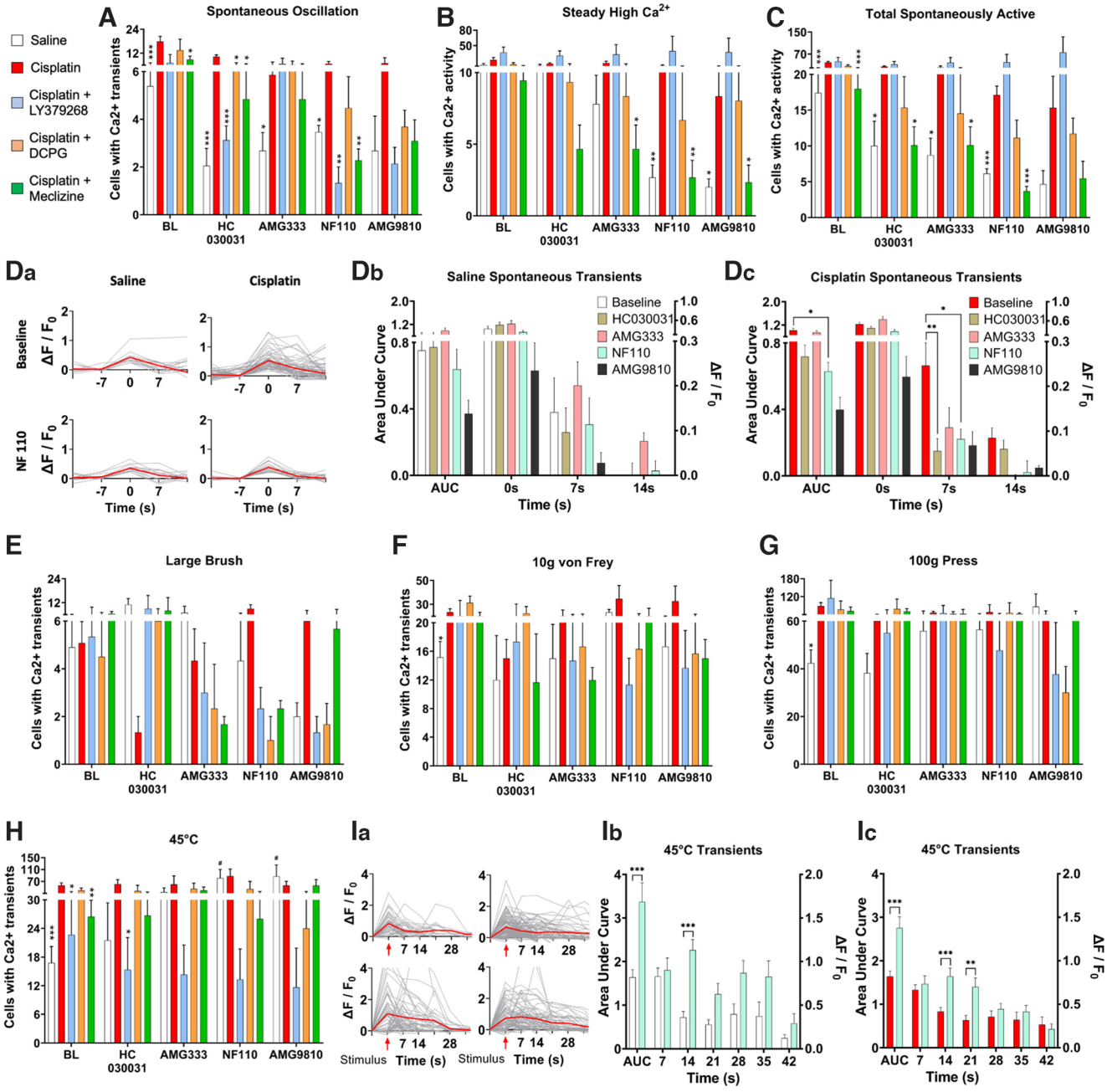

Figure 7. TRP channel inhibitors reduce spontaneous Ca^{2+} oscillation and P2X3 inhibitor, NF 110, increases amplitude of Ca^{2+} transients in response to 45°C stimulus. DRGs of animals-treated with saline vehicle, cisplatin, cisplatin plus LY379268, cisplatin plus (S)−3,4-DCPG, and cisplatin plus meclizine were imaged for spontaneous Ca^{2+} activity in the absence of stimuli, and cells with Ca^{2+} oscillation and steady-state high Ca^{2+} were counted. TRP channel inhibitors were topically applied to the DRGs, and the imaging process was repeated with three to four PBS washes between drug applications. Inhibitors and their targets were HC 030031 (TRPA1), AMG 333 (TRPM8), NF 110 (P2X3 and P2X2/3 heteromultimers), and AMG 9810 (TRPV1). ***A–C***, Graphs show numbers of cells producing Ca^{2+} transients spontaneously in the absence of stimuli, steady-state high cytosol Ca^{2+}, and total spontaneously Ca^{2+} active cells. ***Da***, Graphs of DRG neurons of animals-treated with saline or cisplatin before and after NF 110 application. Spontaneous Ca^{2+} transients are shown with maximum fluorescence intensity set at 0 s. *Y*-axis, $\Delta F/F_0$ fluorescence intensity. ***Db***, ***Dc***, Mean fluorescence intensities of spontaneous Ca^{2+} transients are shown as a function of time frame in saline-treated, and cisplatin-treated animals. Left *y*-axis, AUC, arbitrary units. Right *y*-axis, $\Delta F/F_0$ fluorescence intensity. ***E–H***, Mice from panels ***A–C*** were subjected to hindpaw stimuli before and after application of each inhibitor to DRG. Graphs show numbers of cells producing Ca^{2+} transients in response to large brush, 10-g von Frey, 100-g press, and paw immersion in 45°C water. For baseline, HC 030031, AMG 333, NF 110, and AMG 9810 cell numbers were, respectively: saline, $n = 10$, 10, 13, 5, and 6 cells and 15, 28, 28, 13, and 10 transients; and cisplatin $n = 18$, 19, 7, 13, and 16 cells and 56, 28, 15, 21, and 14 transients. ***Ia***, Graphs of DRG neuronal Ca^{2+} transits of animals treated with saline or cisplatin before and after NF 110 application. Ca^{2+} transients in response to paw immersion in 45°C water are shown, maximum fluorescence intensity is set at 0 s. *Y*-axis, $\Delta F/F_0$ fluorescence intensity. For baseline, HC 030031, AMG 333, NF 110, and AMG 9810, numbers of cells were, respectively: saline, $n = 44$, 61, 86, 60, and 60 cells and cisplatin, $n = 135$, 92, 120, 86, and 80 cells. ***Ib***, ***Ic***, Mean fluorescence intensities of Ca^{2+} transients in response to paw immersion in 45°C water as a function of time frame in saline vehicle-treated (***Ib***) and cisplatin-treated animals (***Ic***) before and after NF 110 treatment. Left *y*-axis, AUC, arbitrary units. Right *y*-axis, $\Delta F/F_0$ fluorescence intensity. Numbers of DRG analyzed for cell counts are shown in Table 4. All graphs show mean ± SEM. Comparisons of cell counts before and after inhibitor application (within treatment groups vs baseline) and for each inhibitor (between treatment groups vs cisplatin) were performed using one-way ANOVA followed by Dunnett's *post hoc* test. AUC and Ca^{2+} transient $\Delta F/F_0$ fluorescence intensity comparisons versus no inhibitor baseline were performed using two-way ANOVA followed by *post hoc* Dunnett's test. $^*p < 0.05$, $^{**}p < 0.01$, $^{***}p < 0.001$. Cell counts compared with baseline before inhibitor treatments; $\#p < 0.05$.

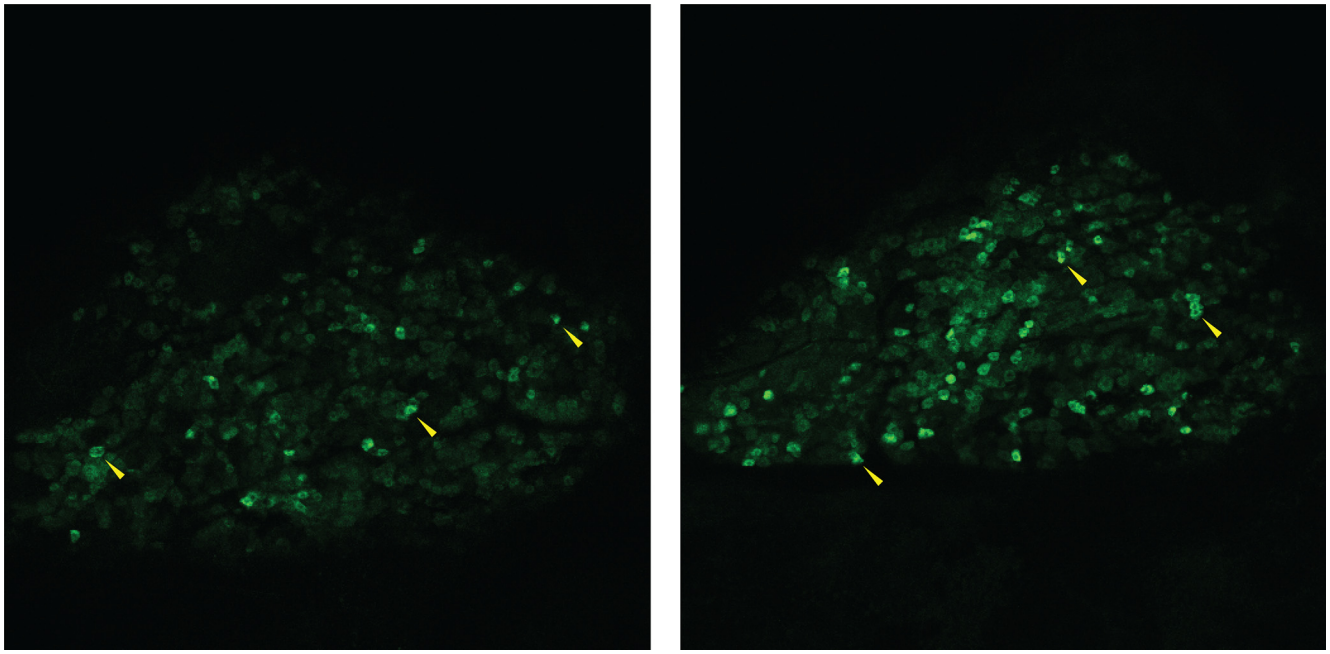

Movie 1. Cisplatin dramatically increases the number of DRG neurons responding to mechanical stimulus. Representative movies generated from microscope images compare DRGs during 100-g press between saline-treated and cisplatin-treated animals. In response to a non-noxious press (100 g), an average of 42.38 cells produced Ca^{2+} transients in saline-treated animals (***A***), and an average of 88.44 cells did so in cisplatin-treated animals (***B***). Arrows show examples of activating neurons. [View online]

The effect of (S)−3,4-DCPG on cisplatin-induced CIPN pain does not appear to be mediated by DRG neurons. mGluR8 is present in most DRG (Carlton and Hargett, 2007; Govea et al., 2012) and trigeminal ganglia (Boye Larsen et al., 2014) neurons. However, the role of mGluR8 in the DRG in CIPN has not been determined. Peripheral administration of mGluR8 agonists (such as (S)−3,4-DCPG) can attenuate thermal and mechanical hyperalgesia caused by carrageenan, formalin, and capsaicin (Marabese et al., 2007; Govea et al., 2012; Pereira and Goudet, 2018). (S)−3,4-DCPG can modulate pain centrally, as well. Infusion of (S)−3,4-DCPG into the periaqueductal gray area was sufficient to reduce nociceptive responses and thermal and mechanical hypersensitivity caused by formalin and carrageenan injection. In addition, infusion of an antagonist of Group III mGluRs to the periaqueductal gray area reduced the analgesic effect of peripheral (S)−3,4-DCPG, showing that mGluR8 can act fully or partially through a central anti-nociceptive pathway (Marabese et al., 2007). Administration of mGluR8 agonist (S)−3,4-DCPG 30 min before cisplatin produced a striking reduction in cisplatin-induced mechanical hypersensitivity and reduced thermal hypersensitivity; yet, (S)−3,4-DCPG-treated animals were not distinguishable in terms of numbers of cells with spontaneous Ca^{2+} activity or numbers of activated cells responding to any stimulus analyzed in this study except 0°C, where (S)−3,4-DCPG increased the number of responding neurons. While there were some subtle differences in Ca^{2+} transients, (S)−3,4-DCPG failed to produce the striking effects on DRG neuronal Ca^{2+} activity seen with LY379268 and meclizine. Since (S)−3,4-DCPG administration was systemic, it was not possible to distinguish central and peripheral effects. The lack of striking decreases in numbers of spontaneously Ca^{2+}-activated neurons or activation from stimuli combined with known effects of (S)−3,4-DCPG in the periaqueductal gray area suggests that attenuation of cisplatin-induced mechanical and thermal hypersensitivity by (S)−3,4-DCPG is central rather than peripheral or that (S)−3,4-DCPG works peripherally through a mechanism that does not affect DRG neuronal Ca^{2+} activity. mGluR8 may be a target for CIPN pain although it does not seem to act peripherally.

Group II mGluR agonists attenuate hyperalgesia and allodynia from a broad range of causes (Carlton et al., 2009; Davidson et al., 2016; Johnson et al., 2017; Mazzitelli et al., 2018; Sheahan et al., 2018), and antagonists of Group II receptors may aggravate hyperalgesia and allodynia, block analgesia, and prolong recovery time from these conditions (Yang and Gereau, 2002, 2003; Zhuo et al., 2016), and may increase the number of action potentials in primary sensory neurons in response to capsaicin or heat (Carlton et al., 2011). Group II mGluRs (mGluR2/3) are broadly expressed in primary sensory neurons (Carlton and Hargett, 2007; Boye Larsen et al., 2014; Sheahan et al., 2018). Our data show that in this cisplatin-induced CIPN model, mGluR2/3 agonist LY379268 reduces mechanical and thermal hyperalgesia and decreases the number of DRG neurons exhibiting spontaneous Ca^{2+} activity as well as the number of DRG neurons producing Ca^{2+} transients in response to 45°C. Mechanical and thermal sensitivity assays were based on systemic administration, so it is not possible to determine the extent to which the effect was peripheral or central. However, reduced numbers of DRG Ca^{2+}-activated neurons indicates that analgesia via primary sensory neuron activity is one mechanism. Other studies have shown peripheral mGluR2 or mGluR2/3 agonists can block inflammatory hyperalgesia (Yang and Gereau, 2002, 2003; Yamamoto et al., 2007). Side effects remain a major concern for Group II mGluR agonists, as convulsions have been observed in preclinical animal models (Dunayevich et al., 2008). Limiting a mGluR2/3 drug to the periphery may reduce side effects (Chishty et al., 2001; Gao et al., 2017; Fan et al., 2018). Our results combined with earlier research suggest that a mGluR2/3 agonist with poor blood brain barrier penetration could treat CIPN pain without disrupting mGluR2/3 signaling in the central nervous system.

Concomitant meclizine treatment reduces mechanical and thermal hyperalgesia and decreases the number of DRG neurons exhibiting spontaneous Ca^{2+} activity (both Ca^{2+} oscillation and

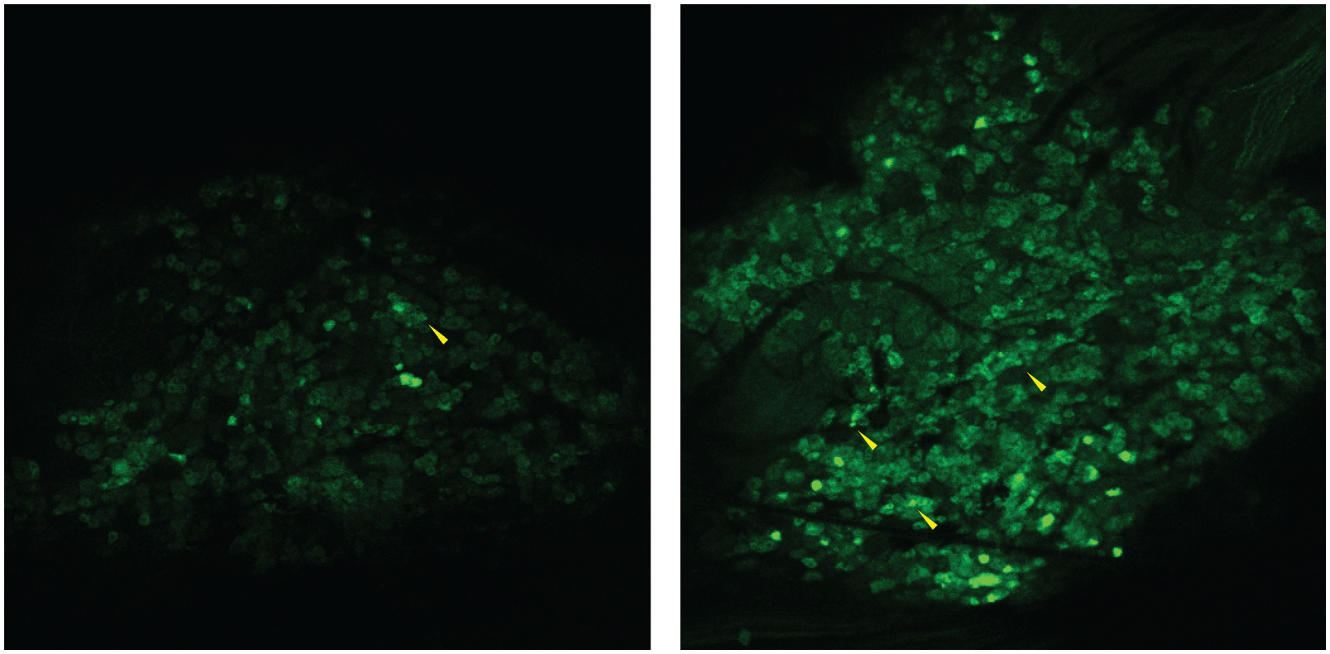

Movie 2. Cisplatin increases the number of cells showing spontaneous Ca^{2+} transients. Representative movies generated from microscope images compare DRGs in the absence of stimuli. An average of 2.39 cells spontaneously produced Ca^{2+} transients in saline-treated animals (***A***) and an average of 17.87 cells produced Ca^{2+} transients in cisplatin-treated animals (***B***). Arrows show examples of activating neurons. [View online]

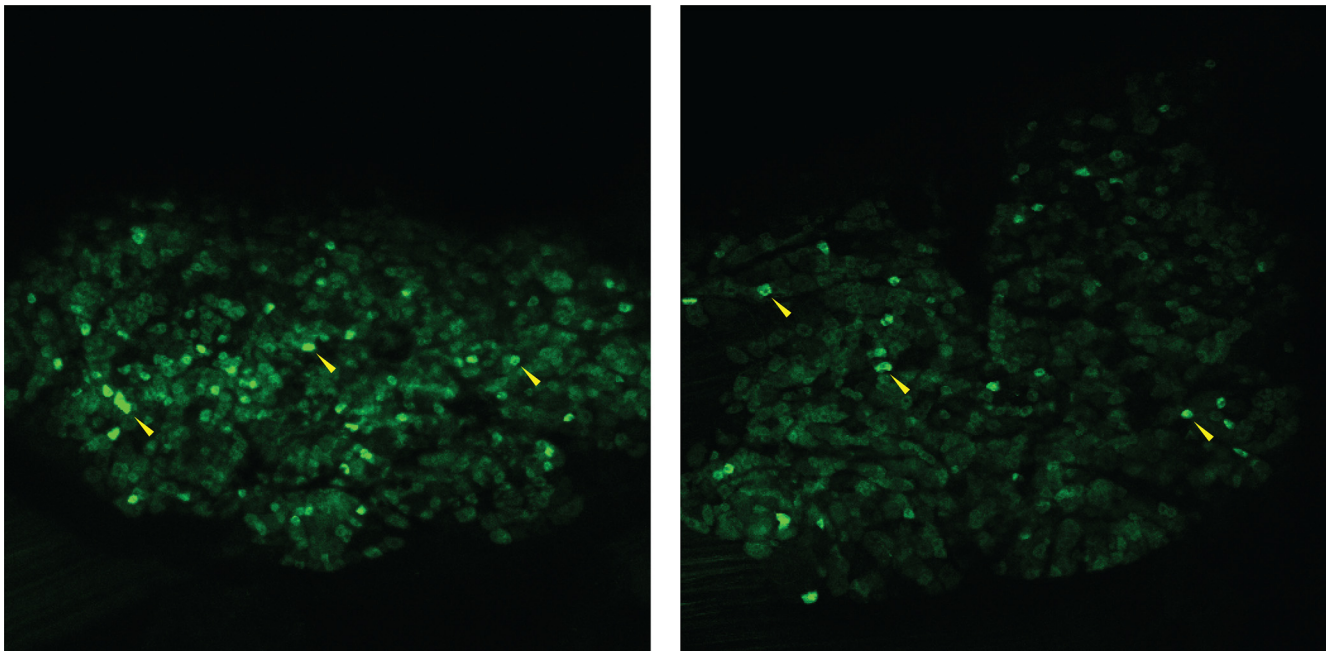

Movie 3. Meclizine dramatically decreases the number of DRG neurons responding to paw immersion in 45°C water in cisplatin-treated animals. In animals treated with cisplatin, an average of 56.88 neurons showed Ca^{2+} transients in response to 45°C hot stimulus (***A***). Treatment with meclizine 3 h prior to cisplatin injection decreased the average number of activated DRG neurons to 26.44 (***B***). Arrows show examples of activating neurons. [View online]

total cells with steady-state high Ca^{2+} activity) and reduces the number of DRG neurons producing Ca^{2+} transients in response to 45°C. Meclizine also reduced the intensity of Ca^{2+} transients arising from two different mechanical stimuli: 10-g von Frey and 100-g press, suggesting that meclizine may act on mechanical pain by reducing the activity of neurons responding to stimuli. Because meclizine treatment was systemic, it is impossible to distinguish a central from peripheral effect. However, there are good reasons to believe that meclizine acts via peripheral mitochondrial repair and/or by reducing oxidative stress. Cisplatin binds mitochondrial DNA in DRG neurons, inhibiting mitochondrial transcription and replication, and causing mitochondrial DNA degradation (Podratz et al., 2011). Cisplatin directly inhibits mitochondrial respiration system *in vivo* and reduces transcription and increases degradation of mitochondrial RNA (Garrido et al., 2008). Meclizine improves clearance of damaged

mitochondrial DNA (Gorgun et al., 2017) and shifts mitochondrial respiration toward glycolytic metabolism (Hong et al., 2016; Zhuo et al., 2016). Meclizine also maintains an elevated ratio of reduced:oxidized glutathione and NADPH (Zhuo et al., 2016; Gorgun et al., 2017). Thus, meclizine employs multiple mechanisms to protect neurons from oxidative damage. ROS and oxidative stress are known to activate and/or potentiate a variety of transient receptor potential channels (Mori et al., 2016; Carrasco et al., 2018), which may partially depolarize neurons, thus rendering them more excitable and resulting in increased spontaneous Ca^{2+} activity and decreased neuron firing threshold in response to stimuli. ROS also affect potassium and sodium channels (Annunziato et al., 2002; Sahoo et al., 2014) and can damage a wide range of other molecules in the cell (Juan et al., 2021). By improving the redox state, enhancing DNA repair, and shifting primary sensory neuron metabolism away from mitochondrial respiration and toward glycolysis, meclizine may attenuate hyperexcitability through multiple known mechanisms, and thereby reduce hypersensitivity to painful stimuli. Meclizine is also an approved drug for use in humans, making it an excellent candidate for possible use in treating CIPN.

One of the more common side effects of platinum-based chemotherapeutic drugs is weight loss (Langer et al., 2002; Fearon et al., 2013; Kazemi-Bajestani et al., 2016). Numerous mechanisms by which cisplatin and other platinum-based chemotherapeutic drugs cause weight loss have been proposed (Yakabi et al., 2010; Hiura et al., 2012; Garcia et al., 2013; Matsumura et al., 2013; Yoshimura et al., 2013; Woo et al., 2016; Guo et al., 2018; Wong et al., 2020). Meclizine reduced both cisplatin-induced hypersensitivity to mechanical pain and cisplatin-induced weight loss. There were no detectable effects of (S)−3,4-DCPG on body weight of cisplatin-treated animals. Of relevance, meclizine is commonly used for treatment of nausea and vomiting during pregnancy (Heitmann et al., 2016) and motion sickness (Paule et al., 2004), and cisplatin induces nausea in humans (Dilruba and Kalayda, 2016). Meclizine is known to be a strong antagonist of H_1 histamine receptor, a weak antagonist of muscarinic acetylcholine receptor (Kubo et al., 1987), and, in mice but not in humans, a weak antagonist of constitutive androstane receptor (Huang et al., 2004). Histamine suppresses food intake in the central nervous system (Clineschmidt and Lotti, 1973; Provensi et al., 2016), and histaminergic neurons play a large role in food intake, metabolism, weight gain or loss, and foraging-related locomotor activities (Provensi et al., 2016). Mice lacking the muscarinic three acetylcholine receptor eat less and weigh less than wild-type mice (Yamada et al., 2001; Gautam et al., 2006). Stimulation of hypothalamic muscarinic acetylcholine receptors stimulates food intake (Jeong et al., 2017). These observations suggest that meclizine may attenuate weight loss through antagonism of anorexigenic H_1 histamine receptors or muscarinic acetylcholine receptors.

We investigated specific receptor roles in our imaging system by applying specific TRP channel inhibitors to DRG cell bodies. Unsurprisingly, the inhibitors decreased the number of spontaneously activating cells. The P2X3 and P2X2/3 heteromultimer inhibitor, NF 110, appeared to sensitize DRGs to 45°C stimulus, increasing the number of cells responding in saline injected control animals and dramatically increasing the fluorescence intensity of Ca^{2+} transients in both cisplatin-injected and saline-injected animals. No TRP channel inhibitors decreased cisplatin-induced sensitivity to stimuli. TRPV1 inhibitor, AMG 9810, also increased the number of Ca^{2+}-activated cells responding to 45°C stimulus. These 45°C stimulus results seem paradoxical, but the inhibitor screen was for indirect effects on stimuli. Inhibitors were applied to the cell bodies rather than into the hindpaw where the receptors that respond directly to the stimuli are found. Importantly, these effects were detectable in saline-treated control animals, but not in cisplatin-treated or cisplatin-plus-TRP channel inhibitor-treated animals. These results suggest that P2X3-injected and TRPV1-induced sensitization is either blocked by, downstream of, or redundant with the effects of cisplatin.

We have used a cisplatin-based CIPN model to study DRG neurons *in vivo* at the level of an intact neuronal ensemble. We found that two (LY379268 and meclizine) of three drug treatments tested attenuated CIPN-induced pain hypersensitivity, reduced spontaneous DRG neuron Ca^{2+} activity, and reduced the number of cells responding to 45°C stimulus. The third drug, (S)−3,4-DCPG, did not reduce spontaneous Ca^{2+} activity, but (S)−3,4-DCPG is known to reduce pain hypersensitivity centrally in some inflammatory pain models. Finally, our results demonstrate that *in vivo* Ca^{2+} imaging of DRG neurons can be used to study mechanisms of CIPN and peripherally-acting candidates for therapeutic intervention.

References

Addington J, Freimer M (2016) Chemotherapy-induced peripheral neuropathy: an update on the current understanding. F1000Res 5:1466.

Anand U, Otto WR, Anand P (2010) Sensitization of capsaicin and icilin responses in oxaliplatin treated adult rat DRG neurons. Mol Pain 6:1744-8069-6-82.

Annunziato L, Pannaccione A, Cataldi M, Secondo A, Castaldo P, Di Renzo G, Taglialatela M (2002) Modulation of ion channels by reactive oxygen and nitrogen species: a pathophysiological role in brain aging? Neurobiol Aging 23:819–834.

Armstrong-Gordon E, Gnjidic D, McLachlan AJ, Hosseini B, Grant A, Beale PJ, Wheate NJ (2018) Patterns of platinum drug use in an acute care setting: a retrospective study. J Cancer Res Clin Oncol 144:1561–1568.

Bhave G, Karim F, Carlton SM, Gereau RW 4th (2001) Peripheral group I metabotropic glutamate receptors modulate nociception in mice. Nat Neurosci 4:417–423.

Boye Larsen D, Ingemann Kristensen G, Panchalingam V, Laursen JC, Nørgaard Poulsen J, Skallerup Andersen M, Kandiah A, Gazerani P (2014) Investigating the expression of metabotropic glutamate receptors in trigeminal ganglion neurons and satellite glial cells: implications for craniofacial pain. J Recept Signal Transduct Res 34:261–269.

Calls A, Carozzi V, Navarro X, Monza L, Bruna J (2020) Pathogenesis of platinum-induced peripheral neurotoxicity: insights from preclinical studies. Exp Neurol 325:113141.

Calls A, Torres-Espin A, Navarro X, Yuste VJ, Udina E, Bruna J (2021) Cisplatin-induced peripheral neuropathy is associated with neuronal senescence-like response. Neuro Oncol 23:88–99.

Carlton SM, Hargett GL (2007) Colocalization of metabotropic glutamate receptors in rat dorsal root ganglion cells. J Comp Neurol 501:780–789.

Carlton SM, Du J, Zhou S (2009) Group II metabotropic glutamate receptor activation on peripheral nociceptors modulates TRPV1 function. Brain Res 1248:86–95.

Carlton SM, Zhou S, Govea R, Du J (2011) Group II/III metabotropic glutamate receptors exert endogenous activity-dependent modulation of TRPV1 receptors on peripheral nociceptors. J Neurosci 31:12727–12737.

Carrasco C, Naziroğlu M, Rodríguez AB, Pariente JA (2018) Neuropathic pain: delving into the oxidative origin and the possible implication of transient receptor potential channels. Front Physiol 9:95.

Chiechio S, Copani A, Zammataro M, Battaglia G, Gereau RW 4th, Nicoletti F (2010) Transcriptional regulation of type-2 metabotropic glutamate receptors: an epigenetic path to novel treatments for chronic pain. Trends Pharmacol Sci 31:153–160.

Chisholm KI, Khovanov N, Lopes DM, La Russa F, McMahon SB (2018) Large scale in vivo recording of sensory neuron activity with GCaMP6. eNeuro 5:ENEURO.0417-17.2018.

Chishty M, Reichel A, Siva J, Abbott NJ, Begley DJ (2001) Affinity for the P-glycoprotein efflux pump at the blood-brain barrier may explain the lack of CNS side-effects of modern antihistamines. J Drug Target 9:223–228.

Cioroiu C, Weimer LH (2017) Update on chemotherapy-induced peripheral neuropathy. Curr Neurol Neurosci Rep 17:47.

Clineschmidt BV, Lotti VJ (1973) Histamine: intraventricular injection suppresses ingestive behavior of the cat. Arch Int Pharmacodyn Ther 206:288–298.

Davidson S, Golden JP, Copits BA, Ray PR, Vogt SK, Valtcheva MV, Schmidt RE, Ghetti A, Price TJ, Gereau RW 4th (2016) Group II mGluRs suppress hyperexcitability in mouse and human nociceptors. Pain 157:2081–2088.

Deng L, Guindon J, Vemuri VK, Thakur GA, White FA, Makriyannis A, Hohmann AG (2012) The maintenance of cisplatin- and paclitaxel-induced mechanical and cold allodynia is suppressed by cannabinoid CB_2 receptor activation and independent of CXCR4 signaling in models of chemotherapy-induced peripheral neuropathy. Mol Pain 8:71.

Descoeur J, Pereira V, Pizzoccaro A, Francois A, Ling B, Maffre V, Couette B, Busserolles J, Courteix C, Noel J, Lazdunski M, Eschalier A, Authier N, Bourinet E (2011) Oxaliplatin-induced cold hypersensitivity is due to remodelling of ion channel expression in nociceptors. EMBO Mol Med 3:266–278.

Dilruba S, Kalayda GV (2016) Platinum-based drugs: past, present and future. Cancer Chemother Pharmacol 77:1103–1124.

Doherty EM, Fotsch C, Bo Y, Chakrabarti PP, Chen N, Gavva N, Han N, Kelly MG, Kincaid J, Klionsky L, Liu Q, Ognyanov VI, Tamir R, Wang X, Zhu J, Norman MH, Treanor JJ (2005) Discovery of potent, orally available vanilloid receptor-1 antagonists. Structure-activity relationship of N-aryl cinnamides. J Med Chem 48:71–90.

Dunayevich E, Erickson J, Levine L, Landbloom R, Schoepp DD, Tollefson GD (2008) Efficacy and tolerability of an mGlu2/3 agonist in the treatment of generalized anxiety disorder. Neuropsychopharmacology 33:1603–1610.

Fan J, Yang J, Jiang Z (2018) Prediction of central nervous system side effects through drug permeability to blood-brain barrier and recommendation algorithm. J Comput Biol 25:435–443.

Fearon K, Arends J, Baracos V (2013) Understanding the mechanisms and treatment options in cancer cachexia. Nat Rev Clin Oncol 10:90–99.

Flatters SJL, Dougherty PM, Colvin LA (2017) Clinical and preclinical perspectives on chemotherapy-induced peripheral neuropathy (CIPN): a narrative review. Br J Anaesth 119:737–749.

Gao Z, Chen Y, Cai X, Xu R (2017) Predict drug permeability to blood-brain-barrier from clinical phenotypes: drug side effects and drug indications. Bioinformatics 33:901–908.

Garcia JM, Scherer T, Chen JA, Guillory B, Nassif A, Papusha V, Smiechowska J, Asnicar M, Buettner C, Smith RG (2013) Inhibition of cisplatin-induced lipid catabolism and weight loss by ghrelin in male mice. Endocrinology 154:3118–3129.

Garrido N, Pérez-Martos A, Faro M, Lou-Bonafonte JM, Fernández-Silva P, López-Pérez MJ, Montoya J, Enríquez JA (2008) Cisplatin-mediated impairment of mitochondrial DNA metabolism inversely correlates with glutathione levels. Biochem J 414:93–102.

Gautam D, Gavrilova O, Jeon J, Pack S, Jou W, Cui Y, Li JH, Wess J (2006) Beneficial metabolic effects of M3 muscarinic acetylcholine receptor deficiency. Cell Metab 4:363–375.

Glimelius B, Manojlovic N, Pfeiffer P, Mosidze B, Kurteva G, Karlberg M, Mahalingam D, Buhl Jensen P, Kowalski J, Bengtson M, Nittve M, Näsström J (2018) Persistent prevention of oxaliplatin-induced peripheral neuropathy using calmangafodipir (PledOx(®)): a placebo-controlled randomised phase II study (PLIANT). Acta Oncol 57:393–402.

Gohil VM, Offner N, Walker JA, Sheth SA, Fossale E, Gusella JF, MacDonald ME, Neri C, Mootha VK (2011) Meclizine is neuroprotective in models of Huntington's disease. Hum Mol Genet 20:294–300.

Gorgun MF, Zhuo M, Englander EW (2017) Cisplatin toxicity in dorsal root ganglion neurons is relieved by meclizine via diminution of mitochondrial compromise and improved clearance of DNA damage. Mol Neurobiol 54:7883–7895.

Govea RM, Zhou S, Carlton SM (2012) Group III metabotropic glutamate receptors and transient receptor potential vanilloid 1 co-localize and interact on nociceptors. Neuroscience 217:130–139.

Greystoke A, Steele N, Arkenau HT, Blackhall F, Md Haris N, Lindsay CR, Califano R, Voskoboynik M, Summers Y, So K, Ghiorghiu D, Dymond AW, Hossack S, Plummer R, Dean E (2017) SELECT-3: a phase I study of selumetinib in combination with platinum-doublet chemotherapy for advanced NSCLC in the first-line setting. Br J Cancer 117:938–946.

Guo F, Gao S, Xu L, Sun X, Zhang N, Gong Y, Luan X (2018) Arcuate nucleus orexin-A signaling alleviates cisplatin-induced nausea and vomiting through the paraventricular nucleus of the hypothalamus in rats. Front Physiol 9:1811.

Hausmann R, Rettinger J, Gerevich Z, Meis S, Kassack MU, Illes P, Lambrecht G, Schmalzing G (2006) The suramin analog 4,4',4",4"'-(carbonylbis(imino-5,1,3-benzenetriylbis (carbonylimino)))tetra-kis-benzenesulfonic acid (NF110) potently blocks P2X3 receptors: subtype selectivity is determined by location of sulfonic acid groups. Mol Pharmacol 69:2058–2067.

Heitmann K, Solheimsnes A, Havnen GC, Nordeng H, Holst L (2016) Treatment of nausea and vomiting during pregnancy -a cross-sectional study among 712 Norwegian women. Eur J Clin Pharmacol 72:593–604.

Hiura Y, Takiguchi S, Yamamoto K, Kurokawa Y, Yamasaki M, Nakajima K, Miyata H, Fujiwara Y, Mori M, Doki Y (2012) Fall in plasma ghrelin concentrations after cisplatin-based chemotherapy in esophageal cancer patients. Int J Clin Oncol 17:316–323.

Hong CT, Chau KY, Schapira AH (2016) Meclizine-induced enhanced glycolysis is neuroprotective in Parkinson disease cell models. Sci Rep 6:25344.

Horne DB, et al. (2018) Discovery of TRPM8 antagonist (S)-6-(((3-fluoro-4-(trifluoromethoxy)phenyl)(3-fluoropyridin-2-yl)methyl)carbamoyl) nicotinic acid (AMG 333), a clinical candidate for the treatment of migraine. J Med Chem 61:8186–8201.

Hu LY, Zhou Y, Cui WQ, Hu XM, Du LX, Mi WL, Chu YX, Wu GC, Wang YQ, Mao-Ying QL (2018) Triggering receptor expressed on myeloid cells 2 (TREM2) dependent microglial activation promotes cisplatin-induced peripheral neuropathy in mice. Brain Behav Immun 68:132–145.

Huang W, Zhang J, Wei P, Schrader WT, Moore DD (2004) Meclizine is an agonist ligand for mouse constitutive androstane receptor (CAR) and an inverse agonist for human CAR. Mol Endocrinol 18:2402–2408.

Ishida H, Zhang Y, Gomez R, Shannonhouse J, Son H, Banik R, Kim YS (2021) In vivo calcium imaging visualizes incision-induced primary afferent sensitization and its amelioration by capsaicin pretreatment. J Neurosci 41:8494–8507.

Jaggi AS, Singh N (2012) Mechanisms in cancer-chemotherapeutic drugs-induced peripheral neuropathy. Toxicology 291:1–9.

Jeong JH, Lee DK, Jo YH (2017) Cholinergic neurons in the dorsomedial hypothalamus regulate food intake. Mol Metab 6:306–312.

Johnson MP, Muhlhauser MA, Nisenbaum ES, Simmons RM, Forster BM, Knopp KL, Yang L, Morrow D, Li DL, Kennedy JD, Swanson S, Monn JA (2017) Broad spectrum efficacy with LY2969822, an oral prodrug of metabotropic glutamate 2/3 receptor agonist LY2934747, in rodent pain models. Br J Pharmacol 174:822–835.

Joseph EK, Chen X, Bogen O, Levine JD (2008) Oxaliplatin acts on IB4-positive nociceptors to induce an oxidative stress-dependent acute painful peripheral neuropathy. J Pain 9:463–472.

Juan CA, P de la Lastra JM, Plou FJ, Pérez-Lebeña E (2021) The chemistry of reactive oxygen species (ROS) revisited: outlining their role in biological macromolecules (DNA, lipids and proteins) and induced pathologies. Int J Mol Sci 22:4642.

Karim F, Wang CC, Gereau RW 4th (2001) Metabotropic glutamate receptor subtypes 1 and 5 are activators of extracellular signal-regulated kinase signaling required for inflammatory pain in mice. J Neurosci 21:3771–3779.

Kazemi-Bajestani SM, Mazurak VC, Baracos V (2016) Computed tomography-defined muscle and fat wasting are associated with cancer clinical outcomes. Semin Cell Dev Biol 54:2–10.

Khasabova IA, Khasabov SG, Olson JK, Uhelski ML, Kim AH, Albino-Ramírez AM, Wagner CL, Seybold VS, Simone DA (2019) Pioglitazone, a PPARγ agonist, reduces cisplatin-evoked neuropathic pain by protecting against oxidative stress. Pain 160:688–701.

Kim YS, Chu Y, Han L, Li M, Li Z, LaVinka PC, Sun S, Tang Z, Park K, Caterina MJ, Ren K, Dubner R, Wei F, Dong X (2014) Central terminal sensitization of TRPV1 by descending serotonergic facilitation modulates chronic pain. Neuron 81:873–887.

Kim YS, Anderson M, Park K, Zheng Q, Agarwal A, Gong C, Saijilafu, Young L, He S, LaVinka PC, Zhou F, Bergles D, Hanani M, Guan Y, Spray DC, Dong X (2016) Coupled activation of primary sensory neurons contributes to chronic pain. Neuron 91:1085–1096.

Kubo N, Shirakawa O, Kuno T, Tanaka C (1987) Antimuscarinic effects of antihistamines: quantitative evaluation by receptor-binding assay. Jpn J Pharmacol 43:277–282.

Kucharczyk MW, Chisholm KI, Denk F, Dickenson AH, Bannister K, McMahon SB (2020) The impact of bone cancer on the peripheral encoding of mechanical pressure stimuli. Pain 161:1894–1905.

Langer CJ, Manola J, Bernardo P, Kugler JW, Bonomi P, Cella D, Johnson DH (2002) Cisplatin-based therapy for elderly patients with advanced non-small-cell lung cancer: implications of Eastern Cooperative Oncology Group 5592, a randomized trial. J Natl Cancer Inst 94:173–181.

Laumet G, Bavencoffe A, Edralin JD, Huo XJ, Walters ET, Dantzer R, Heijnen CJ, Kavelaars A (2020) Interleukin-10 resolves pain hypersensitivity induced by cisplatin by reversing sensory neuron hyperexcitability. Pain 161:2344–2352.

Marabese I, de Novellis V, Palazzo E, Scafuro MA, Vita D, Rossi F, Maione S (2007) Effects of (S)-3,4-DCPG, an mGlu8 receptor agonist, on inflammatory and neuropathic pain in mice. Neuropharmacology 52:253–262.

Masuoka T, Yamashita Y, Yoshida J, Nakano K, Tawa M, Nishio M, Ishibashi T (2020) Sensitization of glutamate receptor-mediated pain behaviour via nerve growth factor-dependent phosphorylation of transient receptor potential V1 under inflammatory conditions. Br J Pharmacol 177:4223–4241.

Matsumura T, Arai M, Yoshikawa M, Sudo K, Nakamura K, Katsuno T, Kanai F, Yamaguchi T, Yokosuka O (2013) Changes in plasma ghrelin and serum leptin levels after Cisplatin-based transcatheter arterial infusion chemotherapy for hepatocellular carcinoma. ISRN Gastroenterol 2013:1–6.

Mazzitelli M, Palazzo E, Maione S, Neugebauer V (2018) Group II metabotropic glutamate receptors: role in pain mechanisms and pain modulation. Front Mol Neurosci 11:383.

McCord JM, Fridovich I (1988) Superoxide dismutase: the first twenty years (1968-1988). Free Radic Biol Med 5:363–369.

McNamara CR, Mandel-Brehm J, Bautista DM, Siemens J, Deranian KL, Zhao M, Hayward NJ, Chong JA, Julius D, Moran MM, Fanger CM (2007) TRPA1 mediates formalin-induced pain. Proc Natl Acad Sci U S A 104:13525–13530.

Melli G, Taiana M, Camozzi F, Triolo D, Podini P, Quattrini A, Taroni F, Lauria G (2008) Alpha-lipoic acid prevents mitochondrial damage and neurotoxicity in experimental chemotherapy neuropathy. Exp Neurol 214:276–284.

Mori Y, Takahashi N, Polat OK, Kurokawa T, Takeda N, Inoue M (2016) Redox-sensitive transient receptor potential channels in oxygen sensing and adaptation. Pflugers Arch 468:85–97.

Nawrocki ST, Carew JS, Pino MS, Highshaw RA, Dunner K Jr, Huang P, Abbruzzese JL, McConkey DJ (2005) Bortezomib sensitizes pancreatic cancer cells to endoplasmic reticulum stress-mediated apoptosis. Cancer Res 65:11658–11666.

Palazzo E, Marabese I, Soukupova M, Luongo L, Boccella S, Giordano C, de Novellis V, Rossi F, Maione S (2011) Metabotropic glutamate receptor subtype 8 in the amygdala modulates thermal threshold, neurotransmitter release, and rostral ventromedial medulla cell activity in inflammatory pain. J Neurosci 31:4687–4697.

Paule MG, Chelonis JJ, Blake DJ, Dornhoffer JL (2004) Effects of drug countermeasures for space motion sickness on working memory in humans. Neurotoxicol Teratol 26:825–837.

Pereira V, Goudet C (2018) Emerging trends in pain modulation by metabotropic glutamate receptors. Front Mol Neurosci 11:464.

Podratz JL, Knight AM, Ta LE, Staff NP, Gass JM, Genelin K, Schlattau A, Lathroum L, Windebank AJ (2011) Cisplatin induced mitochondrial DNA damage in dorsal root ganglion neurons. Neurobiol Dis 41:661–668.

Provensi G, Blandina P, Passani MB (2016) The histaminergic system as a target for the prevention of obesity and metabolic syndrome. Neuropharmacology 106:3–12.

Quasthoff S, Hartung HP (2002) Chemotherapy-induced peripheral neuropathy. J Neurol 249:9–17.

Quintão NLM, Santin JR, Stoeberl LC, Corrêa TP, Melato J, Costa R (2019) Pharmacological treatment of chemotherapy-induced neuropathic pain: PPARγ agonists as a promising tool. Front Neurosci 13:907.

Radwani H, Roca-Lapirot O, Aby F, Lopez-Gonzalez MJ, Benazzouz R, Errami M, Favereaux A, Landry M, Fossat P (2017) Group I metabotropic glutamate receptor plasticity after peripheral inflammation alters nociceptive transmission in the dorsal of the spinal cord in adult rats. Mol Pain 13:1744806917737934.

Sahoo N, Hoshi T, Heinemann SH (2014) Oxidative modulation of voltage-gated potassium channels. Antioxid Redox Signal 21:933–952.

Seretny M, Currie GL, Sena ES, Ramnarine S, Grant R, MacLeod MR, Colvin LA, Fallon M (2014) Incidence, prevalence, and predictors of chemotherapy-induced peripheral neuropathy: a systematic review and meta-analysis. Pain 155:2461–2470.

Sheahan TD, Valtcheva MV, McIlvried LA, Pullen MY, Baranger DAA, Gereau RW 4th (2018) Metabotropic glutamate receptor 2/3 (mGluR2/3) activation suppresses TRPV1 sensitization in mouse, but not human, sensory neurons. eNeuro 5:ENEURO.0412-17.2018.

Ta LE, Bieber AJ, Carlton SM, Loprinzi CL, Low PA, Windebank AJ (2010) Transient receptor potential vanilloid 1 is essential for cisplatin-induced heat hyperalgesia in mice. Mol Pain 6:15.

Wong YS, Lin MY, Liu PF, Ko JL, Huang GT, Tu DG, Ou CC (2020) D-methionine improves cisplatin-induced anorexia and dyspepsia syndrome by attenuating intestinal tryptophan hydroxylase 1 activity and increasing plasma leptin concentration. Neurogastroenterol Motil 32:e13803.

Woo SM, Choi YK, Kim AJ, Yun YJ, Shin YC, Cho SG, Ko SG (2016) Sipjeon-dea-bo-tang, a traditional herbal medicine, ameliorates cisplatin-induced anorexia via the activation of JAK1/STAT3-mediated leptin and IL-6 production in the fat tissue of mice. Mol Med Rep 13:2967–2972.

Yakabi K, Sadakane C, Noguchi M, Ohno S, Ro S, Chinen K, Aoyama T, Sakurada T, Takabayashi H, Hattori T (2010) Reduced ghrelin secretion in the hypothalamus of rats due to cisplatin-induced anorexia. Endocrinology 151:3773–3782.

Yamada M, Miyakawa T, Duttaroy A, Yamanaka A, Moriguchi T, Makita R, Ogawa M, Chou CJ, Xia B, Crawley JN, Felder CC, Deng CX, Wess J (2001) Mice lacking the M3 muscarinic acetylcholine receptor are hypophagic and lean. Nature 410:207–212.

Yamamoto T, Saito O, Aoe T, Bartolozzi A, Sarva J, Zhou J, Kozikowski A, Wroblewska B, Bzdega T, Neale JH (2007) Local administration of N-acetylaspartylglutamate (NAAG) peptidase inhibitors is analgesic in peripheral pain in rats. Eur J Neurosci 25:147–158.

Yang D, Gereau RW 4th (2002) Peripheral group II metabotropic glutamate receptors (mGluR2/3) regulate prostaglandin E2-mediated sensitization of capsaicin responses and thermal nociception. J Neurosci 22:6388–6393.

Yang D, Gereau RW 4th (2003) Peripheral group II metabotropic glutamate receptors mediate endogenous anti-allodynia in inflammation. Pain 106:411–417.

Yi LT, Dong SQ, Wang SS, Chen M, Li CF, Geng D, Zhu JX, Liu Q, Cheng J (2020) Curcumin attenuates cognitive impairment by enhancing autophagy in chemotherapy. Neurobiol Dis 136:104715.

Yoshimura M, Matsuura T, Ohkubo J, Ohno M, Maruyama T, Ishikura T, Hashimoto H, Kakuma T, Yoshimatsu H, Terawaki K, Uezono Y, Ueta Y (2013) The gene expression of the hypothalamic feeding-regulating peptides in cisplatin-induced anorexic rats. Peptides 46:13–19.

Zammataro M, Sortino MA, Parenti C, Gereau RW 4th, Chiechio S (2014) HDAC and HAT inhibitors differently affect analgesia mediated by group II metabotropic glutamate receptors. Mol Pain 10:68.

Zhu J, Li P, Zhou YG, Ye J (2020) Altered energy metabolism during early optic nerve crush injury: implications of Warburg-like aerobic glycolysis in facilitating retinal ganglion cell survival. Neurosci Bull 36:761–777.

Zhu Y, Howard GA, Pittman K, Boykin C, Herring LE, Wilkerson EM, Verbanac K, Lu Q (2019) Therapeutic effect of Y-27632 on tumorigenesis and cisplatin-induced peripheral sensory loss through RhoA-NF-κB. Mol Cancer Res 17:1910–1919.

Zhuo M, Gorgun MF, Englander EW (2016) Augmentation of glycolytic metabolism by meclizine is indispensable for protection of dorsal root ganglion neurons from hypoxia-induced mitochondrial compromise. Free Radic Biol Med 99:20–31.